JCI insight

Self-reactive B cells in the GALT are actively curtailed to prevent gut inflammation

Ashima Shukla, Cindi Chen, Julia Jellusova, Charlotte R. Leung, Elaine Kao, Numana Bhat, Wai W. Lin, John R. Apgar, Robert C. Rickert

JCI Insight. 2019. https://doi.org/10.1172/jci.insight.130621.

Research In-Press Preview **Immunology** **Inflammation**

Immune homeostasis in the gut associated lymphoid tissues (GALT) is critical to prevent the development of inadvertent pathologies. B cells as the producers of antibodies and cytokines plays an important role in maintaining the GALT homeostasis. However, the mechanism by which B cells specifically direct their responses towards non-self-antigens and become ignorant to self-antigens in the GALT is not known. Therefore, we developed a novel mouse model by expressing Duck Egg Lysozyme (DEL) in gut epithelial cells in presence of HEL reactive B cells. Notably, we observed a transient activation and rapid deletion of self-reactive B cells in Peyers Patches and Mesenteric lymph nodes upon self-antigen exposure. The survival of self-reactive B cells upon exposure to their self-antigen was partially rescued by blocking receptor editing but could be completely rescued by stronger survival signal like ectopic expression of BCL2. Importantly, rescuing the self-reactive B cells promoted production of auto-antibodies and gut inflammation. Mechanistically, we identify a specific activation of TGFβ signaling in self-reactive B cells in the gut and a critical role of this pathway in maintaining peripheral tolerance. Collectively, our studies describe functional consequences and fate of self-reactive B cells in GALT and provide novel mechanistic insights governing self-tolerance of B cells in the gut.

Self-reactive B cells in the GALT are actively curtailed to prevent gut inflammation.

Ashima Shukla, Ph.D.[1*#], Cindi Chen, M.S.[1*], Julia Jellusova Ph.D.[1], Charlotte R. Leung, M.S.[1], Elaine Kao, Ph.D.[1], Numana Bhat, M.Sc.[1], Wai W. Lin, Ph.D.[1], John R. Apgar, Ph.D.[1] and Robert C. Rickert, Ph.D.[1]

[1]Tumor Microenvironment and Cancer Immunology Program, Sanford Burnham Prebys Medical Discovery Institute, La Jolla, CA.

*Equally contributed authors, [#]Corresponding author

#Address Correspondence to:

Ashima Shukla, Ph.D.

Tumor Microenvironment and Cancer Immunology Program

Sanford Burnham Prebys Medical Discovery Institute

La Jolla, CA 92037

10901 N Torrey Pines Rd

Phone: 858-646-3100 Ext-3487

Fax: 858-795-5412

Email: ashukla@sbpdiscovery.org

Abstract: Immune homeostasis in the gut associated lymphoid tissues (GALT) is critical to prevent the development of inadvertent pathologies. B cells as the producers of antibodies and cytokines plays an important role in maintaining the GALT homeostasis. However, the mechanism by which B cells specifically direct their responses towards non-self-antigens and become ignorant to self-antigens in the GALT is not known. Therefore, we developed a novel mouse model by expressing Duck Egg Lysozyme (DEL) in gut epithelial cells in presence of HEL reactive B cells. Notably, we observed a transient activation and rapid deletion of self-reactive B cells in Peyers Patches and Mesenteric lymph nodes upon self-antigen exposure. The survival of self-reactive B cells upon exposure to their self-antigen was partially rescued by blocking receptor editing but could be completely rescued by stronger survival signal like ectopic expression of BCL2. Importantly, rescuing the self-reactive B cells promoted production of auto-antibodies and gut inflammation. Mechanistically, we identify a specific activation of TGFβ signaling in self-reactive B cells in the gut and a critical role of this pathway in maintaining peripheral tolerance. Collectively, our studies describe functional consequences and fate of self-reactive B cells in GALT and provide novel mechanistic insights governing self-tolerance of B cells in the gut.

Introduction: The mammalian intestine is a complex environment that is continuously exposed to vast variety of antigens (Ags) from commensal and pathogenic microbes as well as dietary factors (1-3). These antigens pose a unique challenge for the innate and adaptive immune system to discriminate between harmful versus innocuous antigens to restrain the spread of pathogenic microbes while also avoiding aberrant inflammatory encounters (4, 5). Immune cells are positioned in the subepithelial layers where they constantly surveil for invading harmful pathogens. The immune system is an integral part of the gut tissue that is required for maintaining its homeostasis. The protective mucus layers along with the secreted immunoglobulins (Ig) particularly IgA, represents critical checkpoints to prevent the entry and spread of pathogenic microbes (6-9). However, under certain pathological conditions, the unrestrained activation of immune responses due to a breach in the mucosal barrier leads to several autoimmune pathologies and perturbation of normal gut homeostasis (2, 10).

B cells are an intricate part gut immunity and also play a pivotal role in the maintenance of intestinal tissue. In the event of a breach in the epithelial barrier, B cells can respond to gut pathogens to prevent dissemination and ultimately resolve infection (11-14). B cells perform these functions by producing Igs as well as several immune modulatory cytokines (12-15). The Ig secreted by plasma cells are captured by poly-Ig receptors on the basolateral surface of the epithelia to mediate endocytosis of Ig complexes that can be cleaved and transported into the apical lumen via transcytosis where, they serve to neutralize the foreign microbes. The Ig-antigen complexes also function to deliver antigens into the subepithelia to presentation to other immune cell subsets regarding the antigenic milieu (7). Moreover, B cells in the gut are potent producers of immune-modulatory cytokines, such as interleukin-10 (IL10), that have pleiotropic effects (16). These immune-modulatory cytokines are important for maintaining the immune homeostasis in the gut associated lymphoid tissues (GALT), blunting excessive inflammatory responses, and regulating the balance between commensal and pathogenic microbes (14-17). Although, B cells are known to be important for maintaining gut homeostasis, the regulation of B cell responses in the gut is incompletely understood.

B cell tolerance mechanisms, which includes clonal deletion, receptor editing and anergy have been well investigated with regard to selection of newly formed B cells in bone marrow (18, 19). However, the tolerance mechanisms that limit self-reactivity to self-antigens expressed in peripheral tissues is less clear. We have previously shown that in the context of an auto-antigen expressed on follicular dendritic cells in the spleen, the self-reactive B cells are rapidly eliminated at the transitional B cell developmental stage to limit self-reactivity (20). Whether similar mechanisms operate in much more convoluted peripheral tissue such as the GALT is not well-studied. In GALT, discrimination of antigens from pathogenic bacteria, beneficial bacteria, food and self-antigen by B cells is vital. Furthermore, in anatomical sites like Peyer's Patches (PPs) and isolated lymphoid follicles, B cells are eliciting an immune response towards pathogenic antigens. The high degree of immune cells activation makes gut predispose to autoimmunity. How B cells make this distinction between self versus non-self at this site is not known. Interestingly, B cells have been shown to express RAG proteins and undergo Ig rearrangements in the lamina propria (LP) but not the PPs during neonatal development in the mouse; an event that coincides with establishment of the microbiota (21). These observations suggest that B cell tolerance appears to occur in the gut where B cells may undergo secondary rearrangements to execute receptor editing and evade reactivity to putative self-antigens. Besides the level of autoantibodies is often elevated in patients with inflamed gut and it is unclear of whether self-reactive B cells initiates the disease or they get recruited at the site upon tissue destruction. Therefore, we wanted to investigate if specific mechanisms exist to render B cells tolerance to self-antigen in the gut.

In our studies, we developed a novel mouse model to study B cell tolerance against the duck egg lysozyme (DEL) as a neo- self-antigen expressed on gut epithelial cells. Strikingly, we observed that the self-reactive B

cells are transiently activated in response to self-antigen before being rapidly eliminated in the PPs and the draining mesenteric lymphnodes (mLNs). The elimination of self-reactive B cells could be rescued by blocking receptor editing or by strong survival signaling like an ectopic overexpression of BCL2, but not by cell-extrinsic survival signals like excessive BAFF. Notably, the rescue of self-reactive B cell survival by expression of BCL2 lead to the production of autoantibodies to HEL, which ultimately progressed to the inflammation in gut and autoantibody production. Transcriptomic analysis revealed specific activation of the transforming growth factor-β (TGFβ) signaling pathway in self-reactive B cells in the GALT and inhibition of this pathway altered the fate of self-reactive B cells in the gut and rescued their survival. To our knowledge this is the first model to study B cell tolerance in GALT. In our model, mature self-reactive B cells gets eliminated in the gut however, the pool in tissues like spleen remains unaltered. Our work defines how B cell tolerance mechanisms operate in the gut to limit self-reactivity and provide mechanistic insights into the molecular pathways regulating these events.

Results:

Self-reactive B cells are eliminated upon antigen encounter in the gut. B cells in gut associated lymphoid tissues (GALT) are constantly exposed to a range of potential antigens; however, the B cell immune responses are kept in check by the induction of peripheral tolerance at steady state. How the peripheral tolerance in gut is induced and maintained remains poorly understood. To gain insights into this process, we generated a model by crossing transgenic mice expressing membrane-bound duck egg lysozyme (mDEL) with mice carrying Villin-cre to obtain Villin^{cre+}mDEL^{loxp} mice. In these mice, upon cre mediated recombination mDEL is expressed uniformly and exclusively throughout the gut epithelial cells including M cells. DEL displays a much lower affinity (~3500-fold, 1.3 x 10^7 M^{-1}) for the HEL-specific BCR that are often used as a model to study central and peripheral tolerance compared to an extraordinarily high affinity exhibited by HEL (4.5 x 10^{10} M^{-1}), which perhaps makes DEL a more physiological model to study tolerance (22, 23). To study the induction of B cell tolerance we further bred the Villin^{cre+}mDEL^{loxp} mice with the SW_{HEL} knock-in mice that generates self-reactive HEL-specific B cells (Figure 1 A). B cells from SW_{HEL} mice express the same rearranged BCR allele as in the MD4 HEL transgenic mice but instead the rearranged HEL-specific allele in SW_{HEL} is targeted into the *IgH* locus. 10-25% of peripheral B cells in adult SW_{HEL} mice display specificity to HEL and undergo receptor editing, normal isotype switching, as well as somatic hypermutation (24).

We first examined whether the expression of DEL in gut epithelia indirectly affects gut microbiome. Fecal samples were collected from mice with several different genotypes including those from the Villin^{cre+}mDEL^{loxp}SW_{HEL} mice and Villin^{cre+}SW_{HEL}, not expressing DEL. (S1 A). Additionally, fecal samples were also obtained from wildtype mice following administration of HEL via oral gavage at multiple time points. Bacterial Genomic DNA was purified from different samples and deep-sequenced for the V4 region of the 16S rRNA gene to measure the diversity of bacterial phyla. The microbial diversity was mostly unaffected by the presence of DEL as a membrane fusion protein, or by acute oral administration of HEL (S1 B). This clearly indicated that perturbance of the gut microbiome is not a cell-extrinsic obfuscating factor of B cell tolerance to DEL as a specific auto-antigen in our model.

Next, to determine the effect of gut associated antigen (mDEL) on the fate of self-reactive B cells, 8-10 weeks old Villin^{cre+}mDEL^{loxp}SW_{HEL} mice and Villin^{cre+}SW_{HEL} mice, which do not express DEL, were analyzed. HEL-specific B cells from spleen, peripheral lymph nodes (pLNs), mesenteric lymph nodes (mLNs) and peyers patches (PPs) were examined. Notably, we observed a striking decrease in HEL-specific cells in PPs (~10 fold), mLNs and pLNs (~6-7 fold) in Villin^{cre+}mDEL^{loxp}SW_{HEL} mice when compared with Villin^{cre+}SW_{HEL} mice. Importantly, no differences in overall frequencies of B cells was observed Figure 1, B and C. These data clearly show a prominent reduction of HEL-specific B cells upon encounter to a gut associated “self-antigen”.

To further elucidate if self-reactive B cells are acutely eliminated upon self-antigen exposure at GALT, adoptive transfers of splenic B cells and bone marrow reconstitution from SW_{HEL} mice into Villin^{cre+} and Villin^{cre+}mDEL^{loxp} mice were performed. Splenic B cells were isolated from SW_{HEL} mice and were labeled with efluor670 dye and

intravenously transferred into Villin^{cre+} and Villin^{cre+}mDEL^{loxp} mice. Two recipient mice from each group were sacrificed on day 1, 3 and 5 post transfer; Followed by the analysis of spleen, pLNs, mLNs and PPs were analyzed. HEL-specific B cells in PPs and pLNs as early as 24 hours post transfer in Villin^{cre+}mDEL^{loxp} mice when compared with Villin^{cre+}, while, the frequencies of HEL-specific cells in spleen and mLNs appeared comparable (S 2). We then analyzed the mice reconstituted with bone marrow cells from SW_{HEL} mice, reconstituted (R)Villin^{cre+} and RVillin^{cre+}mDEL^{loxp}. At 8 weeks post-reconstitution, HEL-specific B cells developed normally in RVillin^{Cre} x mDEL^{loxP} mice and constituted similar frequencies among total B cells when compared with RVillin^{Cre} controls in the spleen (Figure 1, D and E). However, similar to Villin^{cre+}mDEL^{loxp}SW_{HEL} mice, a strong reduction in HEL-specific B cells in the (~2-fold) PPs and (~1.5 fold) pLNs of RVillin^{Cre} x mDEL^{loxP} mice were observed when compared with RVillin^{Cre}. Collectively, these results suggest that HEL-specific self-reactive B cells are specifically eliminated upon encountering their self-antigen in GALT.

HEL-specific self-reactive B cells show an increased turnover rate in PPs. We observed a strong reduction in HEL-specific self-reactive B cells in the GALT in the presence of a gut associated self-antigen, this prompted us to further examine the turnover of HEL-specific cells at these sites. BCR stimulation by their cognate antigens is known to induce cell proliferation. However, whether BCR stimulation in the context of a self-antigen in the gut would induce proliferation of self-reactive B cells is not clear. To test this, we studied the cell kinetics and trafficking of HEL-specific B cells, by continuously feeding Bromodeoxyuridine (BrdU) containing water to Villin^{cre+}mDEL^{loxp}SW_{HEL} and Villin^{Cre+}SW_{HEL} as well as RVillin^{Cre} x mDEL^{loxP} and RVillin^{Cre} mice for 8 weeks. This approach labelled all the proliferating cells with BrdU, and therefore allowed us to determine the rate of replenishment of tissue resident cellular pools. We observed an almost 100 percent labelling of bone marrow cells with BrdU, and we traced the relative frequency of HEL specific, BrdU positive cells in PPs, pLNs, mLNs and spleen as a snapshot to determine the turnover of HEL-specific B cells at these different sites. Notably, ~50% of HEL-specific B cells in the PPs of Villin^{cre+}mDEL^{loxp}SW_{HEL} were labelled with BrdU compared with 25% in Villin^{Cre+}SW_{HEL} mice Figure 2 A. A much weaker trend for BrdU positive HEL-specific B cells was also seen in pLNs, mLNs and spleen of Villin^{cre+}mDEL^{loxp}SW_{HEL} mice. Similar results were observed in RVillin^{Cre} x mDEL^{loxP} and RVillin^{Cre} mice (Figure 2 B). The replenishment of newly formed cells was not observed in non-HEL specific cells (Figure 2 C). These data could be reconciled in two possible ways; either HEL-specific B cells transiently proliferate upon encountering its cognate antigen in GALT or they are constantly replenished by BrdU labelled cells from the bone marrow. To test the first scenario, we isolated and labelled splenic B cells from SW_{HEL} mice with efluoro670 dye to track their proliferation. The labelled B cells were intravenously transferred into Villin^{cre+}mDEL^{loxp} and Villin^{Cre+} mice. However, the proliferation of transferred SW_{HEL} cells in PPs between Villin^{cre+}mDEL^{loxp} and Villin^{Cre+} appeared comparable at day 1, 3 and 5 post-transfer. This suggests that the increased frequency of BrdU positive cells in Villin^{cre+}mDEL^{loxp} did not occur as a consequence of transient antigen driven cellular proliferation (Figure 2 D) but most likely resulted from an intensive replenishment of HEL-specific cells in PP by BrdU labelled B cells from bone marrow.

HEL-specific self-reactive B cells are activated upon antigen encounter in gut associated lymphoid tissues. HEL-specific B cells showed comparable proliferative responses in the presence (Villin^{cre+}mDEL$^{loxp)}$ or absence (Villin^{Cre+}) of its cognate antigen. Therefore, we next analyzed whether HEL-specific B cells display features of cellular activation upon antigen encounter. BCR, upon binding to its antigen, is internalized and as a consequence the cell surface levels of BCR are downregulated. We compared the cell surface levels of HEL binding BCR of HEL-specific self-reactive B cells upon antigen encounter in RVillin^{Cre}mDEL^{loxP} mice. An approximate of 2 and 1.5 fold reduction in the MFI of surface Ig and HEL-specific BCR were observed in mLNs and PPs of RVillin^{Cre}mDEL^{loxP} mice compared with HEL-specific B cells from RVillin^{Cre} (Figure 3, A and B). Moreover, the levels of cell surface Ig and HEL-specific BCR were comparable at lymphoid tissues not expressing the antigen such as pLNs and spleen. We also evaluated the expression of B cell activation markers, CD69 and CD86 on HEL-specific B in the presence or absence of its antigen. We observed an increase in the levels of CD69 and CD86, in PPs and mLNs of RVillin^{Cre}mDEL^{loxP} mice compared with RVillin^{Cre} mice (Figure 3, C and D). Interestingly, the upregulation of CD69, which is considered an early marker of cell activation, was

much more pronounced on HEL-specific B cells in the PPs, while CD86, an activation marker with costimulatory functions, was significantly upregulated in mLNs. These data indicate that HEL-specific B cells upon encountering the self-antigen at the gut epithelia are transiently activated and a subset among these cells traffic to the mLN, where they undergo further activation. Even though the HEL-specific B cells underwent activation, they failed to enter the Germinal Center (GC) reaction as indicated by the lack of GC B marker, GL7 (Figure 3, E and F). Together, these data show that HEL-specific B cells undergo activation upon antigen encounter in the GALT.

Self-reactive B cells undergoes deletion and receptor editing in the GALT. Our results showed that HEL-specific B cells upon binding to self-antigen in GALT undergoes cellular activation and their numbers undergo reduction. This suggests that upon antigen encounter, either majority of HEL-specific B cells in GALT are clonally deleted or are shunted towards a terminal differentiation pathway leading to the generation of short-lived plasma cells. To address these scenarios, we first monitored the production of auto-antibodies specific to HEL by using a flow based assay developed in our laboratory (25). Serum and fecal extracts were collected from RVillin^{Cre+}mDEL^{loxP} and control RVillin^{Cre+} mice then the antibody titers were measured. We did not observe any significant differences in the production of HEL-specific antibodies of IgM, IgG1 and IgA isotypes in the sera and fecal extracts (S3, A and B). These results demonstrate that HEL-specific B cells upon antigen encounter are not channeled towards a terminal plasma cell differentiation pathway.

We then investigated the possibility for clonal elimination of HEL-specific B cells upon encountering self-antigen in GALT. We analyzed several markers associated with cell death on HEL-specific cells from RVillin^{Cre+}mDEL^{loxP} and control RVillin^{Cre+} mice. Notably, HEL-specific cells in PPs and mLNs express significant increase in the pro-apoptotic protein BIM, Figure 4 A and Annexin-V (S3 C). Histological examination of HEL-specific B cells in PPs of RVillin^{Cre+}mDEL^{loxP} also showed higher BIM positivity, Figure 4 B, however the architecture of follicles were retained (S4 F). These results indicate that self-reactive B cells undergo elimination upon encountering its antigen. To test the provision of an external survival signal would prevent the elimination of self-reactive B cells in GALT, we used a human CD68 promoter driven BAFF transgenic mice line and crossed it to SW$_{HEL}$ mice (SW$_{HEL}$*Baff*) (26). BAFF belongs to the TNF superfamily of receptors and is a well-known survival factor for mature B cells in the periphery. The RVillin^{Cre+}mDEL^{loxP} and control, RVillin^{Cre+} mice were then reconstituted by the bone marrow cells from SW$_{HEL}$*Baff* mice (RVillin^{Cre+}mDEL^{loxP}(*Baff*)) and (RVillin^{Cre+}(*Baff*)). Rather surprisingly, even the overexpression of BAFF could not rescue the elimination of HEL-specific cells upon antigen encounter in PPs (S3, D and E). This was particularly intriguing as higher levels of BAFF have been associated with autoimmune diseases including Ulcerative Colitis and Crohn's disease, and BAFF transgenic mice have also been shown to develop autoimmunity (26-28). However, in our experimental system, overexpression of BAFF alone was not sufficient to breach tolerance against a gut associated self-antigen.

SW$_{HEL}$ B cells undergo V_H replacement of the knockin allele, which is the primary reason that only 20-30% of the peripheral B cells are HEL-specific. Therefore, to determine the maximal efficiency of negative selection in the absence of secondary recombination events, we crossed the SW$_{HEL}$ mice onto a *Rag2 null* background to obtain SW$_{HEL}$(*Rag2*^{KO}). In this case, all peripheral B cells bind HEL and allow us to evaluate receptor down modulation and apoptosis in straightforward manner relative to control mice lacking mDEL expression. Next, we reconstituted Villin^{Cre+}mDEL^{loxP} and control, Villin^{Cre+} mice with SW$_{HEL}$(*Rag2*^{KO}) BM to obtain RVillin^{Cre+}mDEL^{loxP}(*Rag2*^{KO}) and control, RVillin^{Cre+}(*Rag2*^{KO}). Remarkably, we observed a partial rescue in the number of HEL specific B cells in PPs indicating an event of receptor editing in self-reactive B cells (Figure 4 C). To confirm, if it is the RAG2 deficiency in self-reactive B cells, leading to rescue we repeated this experiment in mixed BM chimeras of SW$_{HEL}$(*Rag2*^{KO}) and μMT mice to provide a functional pool of T cells. Remarkably, we obtained no difference in the number of HEL-specific B cells in RVillin^{Cre+}mDEL^{loxP}(*Rag2*^{KO}) and control, RVillin^{Cre+}(*Rag2*^{KO}) in the presence of absence of T cells (Figure 4, D and E). These results suggests that upon BCR engagement to self-antigen induces RAG, leading to V_H replacement and a switch in specificity to avoid elimination.

Ectopic expression of BCL2 rescues survival of self-antigen exposed self-reactive B cells. Next we tested, whether a cell intrinsic survival signal is capable of rescuing the survival of HEL-specific B cells in the gut remains unknown. To further investigate this, we crossed the SW_{HEL} mice to the Eμ-*Bcl2*-22 transgenic mice line (SW_{HEL}(*Bcl2*)) to allow B lineage-specific overexpression of the anti-apoptotic protein Bcl-2 (29, 30). We reconstituted RVillin^{Cre} mDEL^{loxP} (RVillin^{Cre}mDEL^{loxP}(*Bcl2*)) and control, RVillin^{Cre} (RVillin^{Cre}(*Bcl2*)) mice with bone marrow cells isolated from SW_{HEL}(*Bcl2*) mice Figure 5 A. Mice were analyzed 8-10 weeks post-reconstitution. Remarkably, ectopic BCL2 expression completely rescued the survival of self-reactive HEL-specific B cells in RVillin^{Cre}mDEL^{loxP}(*Bcl2*) mice compared to RVillin^{Cre}(*Bcl2*) control mice, Figure 5, B and C. Moreover, the BCL2 expressing HEL-specific B cells showed downregulation of cell surface BCR as well as upregulation of CD86 and MHC-II that together represent features associated with cellular activation (Figure 5, D and F). Intriguingly, the protein levels of BIM were still upregulated in BCL2 overexpressing HEL-specific cells (Figure 5 G), consistent with the fact that BCL2 counteracts the activity but not the expression of BIM protein (31). The upregulation of BIM in HEL-specific cells from RVillin^{Cre}mDEL^{loxP}(*Bcl2*) mice also implies that even in the presence of BCL2, HEL-specific self-reactive B cells in the context of a gut associated self-antigen are primed to undergo apoptosis and this process is aborted only by the downstream anti-apoptotic effects of BCL2. Together, these results demonstrate that cell intrinsic survival signals can rescue the terminal fate of self-reactive B cells in the gut.

Breach in B cell peripheral tolerance to gut associated antigen develops gut inflammation. Since, ectopic expression of BCL2 rescued the survival of self-reactive B cells in GALT, we then closely examined the RVillin^{Cre}mDEL^{loxP}(*Bcl2*) mice for apparent signs of pathologies. First, we determine the BCR isotype, self-reactive B cells will switch in gut upon receiving survival signal by surface staining HEL-specific cells. Interestingly, we observed ~2.5 fold increase in HEL-specific IgA expressing cells in the PPs of RVillin^{Cre}mDEL^{loxP}(*Bcl2*) mice compared to the RVillin^{Cre}(*Bcl2*) control mice (Figure 6 A. Second, to determine if the fate of these self-reactive B cells is altered, we measured the BCR specific antibody production in serum and fecal extracts. Interestingly, we observed a significant (~1.5 fold) increase in HEL-specific IgA antibody in the serum and fecal extracts, whereas non-significant increase in HEL-specific IgG1 antibody was observed in serum of RVillin^{Cre}mDEL^{loxP}(*Bcl2*) when compared with RVillin^{Cre}(*Bcl2*) mice (Figure 6, B and C). Remarkably, histological evaluation of the gut in RVillin^{Cre}mDEL^{loxP}(*Bcl2*) mice showed several characteristic features of colonic inflammation that are also associated with human IBD. These included submucosa and muscosa infiltration by lymphocytes, flattening of crypts and in general a higher degree of inflammation, Figure 6, C and D. Notably, these pathologies developed spontaneously, displaying higher pathological scores and the other two mice showing milder but overt signs of pathologies (Table 1). Importantly, none of the RVillin^{Cre}mDEL^{loxP}(*Bcl2*) control mice from the same cohort developed such conditions. Together, these observations suggest that intrinsic survival signals such as those provided by ectopic expression of *Bcl2* causes a breach in peripheral tolerance in the gut leading to development of overt inflammatory pathologies.

Transcriptional profiling of HEL-specific self-reactive B cells reveal upregulation of TGFβ signaling. To elucidate the molecular mechanism involved in rendering B cells tolerant to the self-antigen at the GALT, we performed transcriptional profiling. To do so, HEL-specific and non-HEL-specific B cells were sorted from spleen, mLNs and PPs from three different Villin^{cre+}mDEL^{loxp}SW_{HEL} mice then RNA-Seq was performed. The HEL-specific B cells from spleen were used as controls to demarcate the transcriptional profile in the absence of self-antigen encounter and non-HEL-specific B cells from the spleen, mLNs and PPs served as internal controls for defining tissue specific gene signatures. We first performed hierarchical clustering analysis to identify the relative similarity between the transcriptional profiles of different samples Figure 7 A. As expected, the HEL-specific self-reactive B cells, particularly those from the PPs and mLNs clustered together; while, the non-HEL-specific non-self-reactive B cells from mLN and spleen as well as HEL-specific B cells from the spleen appeared more closely related to one another. The non-HEL-specific B cells in PPs showed some resemblance to HEL-specific B cells in PPs, likely because a subset among these cells undertake a germinal center program and display features of cell activation.

We then compared these data sets in various permutations to first identify differentially expressed gene (DEG) signatures in HEL-specific cells in PPs versus those present in mLNs and spleen. Our analysis identified 591 and 488 DEGs in HEL-specific cells in PPs compared with mLNs and spleen, respectively Figure 7 B. Concurrently, we identified 926 and 862 DEGs in non-HEL-specific cells in PPs compared with mLNs and spleen (S4). We further used the HEL-specific and non-HEL-specific DEG signatures to perform metacore and metascape pathway analysis, which revealed a total of 10 statistically significant unique molecular pathways differentially regulated among self-reactive HEL-specific B cells upon self-antigen exposure in PPs compared with mLN and spleen Figure 7 C. Similarly, a total of 16 differentially regulated molecular pathways were identified among non-HEL-specific B cells in PPs compared with mLNs and spleen and these were used to determine tissue specific changes, Figure 7 D. These uniquely regulated pathways in HEL-specific and non-HEL-specific B cells at PPs were then compared to each other to delineate 8 unique molecular pathways that are specifically enriched among HEL-specific B cells upon self-antigen exposure, Figure 7 E. Notably, among these unique pathways, our analysis revealed significant enrichment of TGFβ signaling induced network in HEL-specific cells in PPs. To investigate this further, we performed a Gene Set Enrichment Analysis (GSEA) using a panel of TGFβ signature genes (identified by treatment of T cells with TGFβ in culture) to test for the enrichment of TGFβ signaling activity in HEL-specific B cells in PPs. Remarkably, we obtained a robust and significant enrichment of TGFβ signature genes among DEGs in HEL-specific B cells in PPs when compared with HEL-specific B cells in spleen Figure 8 A. Moreover, we also observed a trend among DEGs identified upon comparison between HEL-specific and non-HEL-specific B cells at PPs for enrichment of TGFβ signature genes Figure 8 B. Furthermore, we observed the enrichment of TGFβ signature genes in HEL-specific cells from PPs from Villin^{cre+}mDEL^{loxp}SW$_{HEL}$ when compared with HEL-specific cells from Villin^{Cre+}SW$_{HEL}$ by RT-PCR, Figure 8 C. Collectively, using systematic and stringent analysis criteria, our studies revealed specific upregulation of TGFβ signaling pathway in HEL-specific B cells following exposure to self-antigen in GALT.

We also performed transcriptional profiling of HEL-specific B cells isolated from PPs, mLNs and Spleen of RVillin^{Cre}mDEL^{loxP}(*Bcl2*) mice to identify molecular pathways that are deregulated upon breaching of B cell tolerance in the gut. As described above, we identified DEGs in HEL-specific B cells from PPs compared with those in mLNs and spleen. Our analysis revealed a total of 232 genes upregulated and 138 genes downregulated in HEL-specific B cells in the PPs compared with spleen and these were used to perform metacore pathway analysis. Once again, we observed activation of TGFβ signaling pathway in PP HEL-specific B cells (supplementary figure), implying that Bcl2 rescues the survival of self-reactive cells at GALT in a cell-intrinsic manner. We then identified DEGs in HEL-specific cells isolated from RVillin^{Cre}mDEL^{loxP}(*Bcl2*) when compared with HEL-specific cells from Villin^{cre+}mDEL^{loxp}SW$_{HEL}$ mice. Consistent with the development of inflammatory pathologies in RVillin^{Cre}mDEL^{loxP}(*Bcl2*), our analysis unveiled pathways involved in the activation of inflammatory response. The HEL-specific cells from PPs displayed enrichment of an immune network for IgA production, Figure 8, D and E. This is in line with our findings that ectopic expression of *Bcl2* rescues the survival of self-reactive B cells at GALT, induces BCR isotype switch to IgA and cellular differentiation.

Inhibition of TGF beta signaling enhances the survival of the self-reactive B cells after gut associated antigen encounter. Our transcriptional profiling and analysis of HEL-specific self-reactive B cells in GALT showed activation of TGFβ signaling pathway upon self-antigen encounter. TGFβ signaling pathway is induced upon binding of TGFβ to TGFβR1/2 leading to internalization of receptors. To confirm this we stained the HEL-specific cells from RVillin^{Cre}mDEL^{loxP}(*Bcl2*) and RVillin^{Cre}(*Bcl2*), control mice. Interestingly, we observed significant ~2.5- 4 fold downregulation of TGFβR1 in HEL-specific cells from spleen, pLNs, mLNs and PPs (Figure 9 A). This was in line with our previous finding of HEL-specific cells in RVillin^{Cre}mDEL^{loxP}(*Bcl2*) have survival advantage and switch to IgA. We next tested whether inhibition of TGFβ signaling could rescue the survival of self-reactive HEL-specific cells in GALT. For these studies, we took a pharmacological approach and utilized a transforming growth factor beta receptor type 1&2 (TGFBR1/2) specific inhibitor, LY2109761 to inhibit TGFβ signaling. We isolated splenic B cells from SW$_{HEL}$ mice that constituted a mixture of HEL-specific and non-HEL-specific B cells and cultured them in the presence of TGFBR1/2 inhibitor or DMSO for two hours. After two

hours we washed and labelled the TGFBR1/2 inhibitor or DMSO treated cells with cell trace dyes, CFSE and Efluor670 or CTV dye, respectively Figure 9 B. The TGFBR1/2 inhibitor or DMSO treated and differentially labelled cells were then mixed together and intravenously injected into Villin^{cre+}mDEL^{loxp} mice. Mice were analyzed 72 hours post injections for relative proportions of transferred cells in spleen, mLNs, pLNs and PPs. Interestingly, we observed a significantly higher frequencies of HEL-specific B cells treated with TGFBR1/2 inhibitor compared with DMSO treated HEL-specific cells within the spleen, mLNs, pLNs and PPs of the same mice, Figure 9 B. Importantly, the frequencies of non-HEL-specific B cells treated with TGFβR1/2 inhibitor were unaltered when compared with non-HEL-specific B cells treated with DMSO (Figure 9 B). To ratify the activity of drug at 72 hours post injections we measured the levels of p-smad2/3 levels and observed significant ~1.5- 10 fold downregulation in TGFβR1/2 inhibitor treated HEL-specific cells from Spleen, pLNs, mLNs and PPs Figure 9 C. The TGFβR1/2 inhibitor treated HEL-specific cells compared with DMSO treated cells, showed upregulation of CD69, an activation gene known to be suppressed by TGFβ signaling (32), and showed higher levels of cell migration marker, S1PR1 indicating less B cell retention in gut (Figure 9 D). Overall, we observed an increase in frequencies of HEL-specific B cells not just in PPs and mLNs, but also at pLN and spleen suggesting that once rescued, the HEL-specific B cells readily recirculate through secondary lymphoid tissues. Together, our results here demonstrate that inhibition of TGFβ signaling in a B cell-intrinsic manner, rescues the survival of self-reactive B cells in the GALT, demonstrating a critical role for TGFβ signaling in regulating B cell tolerance at GALT.

Discussion.

The GALT is a complex microenvironment, where B cells are challenged by a vast variety of harmless and pathogenic Ags. Our understanding of how B cells discriminate between these different Ags to either become ignorant or generate functional immune responses is quite limited. In our studies here, we developed a novel mouse model to study the interaction of self-reactive B cells with cognate auto-antigen in the gut. Our model mimics physiological scenarios, where only a small fraction (10-20%) of B cells harboring self-reactive BCR that develop in the bone marrow and egress into the periphery. Notably, our studies unraveled robust tolerance mechanisms that rapidly abolished self-reactive B cells in the gut to suppress the development of overt pathologies. While, delivery cell-intrinsic survival signal by ectopic expression of *Bcl2* rescued the terminal fate of auto-reactive B cells and caused inflammation in gut. We performed transcriptomics analysis and used stringently curated filtering criteria to identified specific activation of TGFβ signaling in self-reactive -HEL-specific B cells that contributed to the elimination of self-reactive B cells in the gut. In our studies here we observed the induction of tolerance to an auto-antigen that is expressed on the cell surface of intestinal epithelial cells, it will be interesting to investigate whether similar mechanisms exist to induce tolerance against cross-reactive self-Ags from commensal microbiota and dietary factors in gut.

Our studies reveal that similar to receptor editing and clonal deletion of self-reactive B cells during central tolerance induced in bone marrow, the self-reactive B cells in the gut undergo BCR rearrangement and apoptosis following encounter with its auto-antigen. Therefore, the induction of receptor editing and apoptosis represents the major mechanisms contributing to peripheral tolerance in the gut. Our studies identify PPs as the primary inductive site where B cells are rapidly eliminated. However, how the self-reactive -BCR receives, relays and delivers an apoptotic or BCR rearrangement signal upon auto-antigen encounter in the gut remains unclear. Perhaps, the specific cytokine milieu in the PPs contributes to this outcome where, BCR engagement with an auto-antigen without relevant T cell help translates to propagation of a death signal in self-reactive B cells. Yet, the signal which directs BCR rearrangement in the gut is still not understood.

Mechanistically, our studies identify activation of TGFβ signaling pathway in HEL-specific self-reactive B cells in the gut leading to their rapid elimination. Pharmacological inhibition of TGFβ signaling by using an inhibitor specific to TGFβR1/R2 reversed these phenotypes, promoted the survival of self-reactive B cells in the gut and led to expression of chemokines that allowed homing of self-reactive B cells to other peripheral tissues. TGFβ signaling pathway is shown to have pleotropic effects on B cells (33-40). In mucosal tissues, TGFβ signaling is

known to be crucial for IgA production, where it cooperates with CD40 ligand (CD40L) and other cytokine signals delivered by T cells to induce class switch recombination in B cells (37). In human B cells lines (also in mouse B cells), TGFβ signaling induces apoptosis by repressing the expression of anti-apoptotic protein, BCL-XL and by directly inducing the expression of pro-apoptotic protein PUMA (39, 40). TGFβ signaling induced apoptosis in B cells is shown to occur in an autocrine manner (35, 36) and PP B cells are known to produce significant amounts of TGFβ (33). Whether and how, the TGFβ signaling functions in an autocrine manner in self-reactive HEL-specific B cells to deliver a pro-apoptotic signal still remains unclear. It is worth pointing out that we observed higher mRNA expression of TGFβR1 and TGFβR2 in self-reactive HEL-specific B cells in PPs compared with non-HEL-specific B cells (S6). However, due to lack of appropriate reagents we were not able to test the changes in protein expression of TGFβR1 and TGFβR2. Perhaps the higher levels of TGFβR1 and TGFβR2 makes self-reactive -HEL-specific B cells more sensitive and responsive to TGFβ levels in PPs. Interestingly, a very recent study showed that activation of TGFβ signaling in PP B cells leads to upregulation of Latent TGFβ binding protein, GARP (41) which can induce production of active TGFβ from latent TGFβ in human B cells to boost IgA production (42). Even though, we did not observe any significant differences in the expression of *Lrrc32*, the gene encoding GARP in self-reactive B cells compared with non-self-reactive B cells in PP, it is reasonable to speculate that higher expression of GARP in PP B cells may contribute to higher levels of active TGFβ in the PP tissue microenvironment which may act in a paracrine axis to induce tolerance. Consistent with this notion, GARP was shown to function in a B cell specific manner to regulate the induction of peripheral tolerance in a model of oral sensitization (41). Taken together, our studies presented here highlights TGFβ signaling as a critical checkpoint for induction of peripheral tolerance in self-reactive B cells in the gut. In line with our findings, extrinsic influences like excessive BAFF producing macrophages does not rescue or alters the fate of the self-reactive B cells. However, upon providing the stronger pro-survival signal like BCL2, in RVillin^{Cre}mDEL^{wt}(*Bcl2*) mice, completely rescues self-reactive cells. Besides, not only the activation status was retained, TGFβ signaling pathway was also enriched in HEL-specific cells in PPs. Further, the percentage of BIM positive self-reactive B cells were still significantly high, indicating that BCL2 only rescues the phenotype but not alters BCR signaling downstream. Moreover, the interesting finding of this study is that just upon receiving survival signaling these cells switched to IgA and increase in HEL-specific IgA antibody was observed.

Our studies here demonstrate that B cell intrinsic activation of TGFβ signaling is important for induction of peripheral tolerance in self-reactive B cells. It is important to point out that we did not observe T cell mediated immune responses directed towards mDEL, indicating that mDEL is truly perceived as “self” in our model. These observations also suggest mechanisms of tolerance that involves diverse immune cell subsets. Previous studies have shown important functions of tolerogenic subsets of dendritic cells and T regulatory cells in actively controlling immune responses to self- and commensal- antigens in gut (43, 44). It would be interesting to further investigate the possible interplay between tolerogenic immune cell subsets and induction of B cell tolerance in the GALT. Importantly, a B cell intrinsic breach in tolerance by Bcl2 expression in our model was sufficient to induce an inflammatory phenotype and development of pathologies, indicating that B cells play a prominent role in regulating tolerance to self-antigen(s) in the gut.

We show that ectopic expression of BCL2 rescued the survival of self-reactive B cells. Interestingly, the transcriptomic profiling of BCL2 overexpressing HEL specific B cells still showed activation of TGFβ signaling pathway, suggesting that B cell intrinsic survival signal does not alter the upstream events that leads to induction of TGFβ signaling in self-reactive B cells. Importantly, our results clearly show that breach in tolerance induction by forced expression of BCL2 in B cells triggered a cascade of events that promotes activation of an inflammatory immune signature. These findings strongly suggest that B cells have important immuno-regulatory functions in mucosal tissues. Consistent with our findings, absence of B cells in mice causes alterations in the cytokine milieu of GALT (17) and Rituximab (B cell depleting antibody) treatment in humans has been linked to development of colitis (45). In our studies, breakdown of B cell intrinsic tolerance mechanisms by BCL2 expression caused development of overt inflammation with many of the clinical symptoms commonly associated with diseases like

autoimmune enteropathy and celiac disease in humans. This to our knowledge is the first model to study B cell tolerance to gut associated self-antigens.

In summary, we generated and used a novel mouse model to interrogate B cell specific responses to their cognate auto-antigen in gut. We performed a systematic analysis to describe that B cell responses to an auto-antigen are actively curtailed by cell intrinsic tolerance mechanisms in gut and any breach in this process leads to development of pathologies. We further provide novel insights into the molecular mechanisms that control the induction of peripheral tolerance and identify TGFβ signaling pathway as a critical checkpoint for regulating this process.

Materials and Methods:

Mice: Villin^{cre+}mDEL^{loxp}SW$_{HEL}$ or Villin^{cre+}mDEL^{wt}SW$_{HEL}$ control mice were used in the various experiments. All mice used were kept on a C57/B6 background. To generate the reconstituted Villin^{cre+}mDEL^{loxp} mice (RVillin^{cre+}mDEL^{loxp}) and reconstituted control mice, 8-12 week old Villin^{cre+}mDEL^{loxp} mice were lethally irradiated (10Gy) and reconstituted via iv injection, performed by vivarium staff at Sanford Burnham Prebys Medical Discovery Institute, with ~6-8x10^6 bone marrow cells from SW$_{HEL}$ or SW$_{HEL}$*Rag2*^{KO} or SW$_{HEL}$*Bcl2* or SW$_{HEL}$*Baff* mice. The mice were given antibiotics (5 mL of Sulfamethalazone in autoclaved water) for 4 weeks and regular water for another 4 weeks before use.

Adoptive transfers: For the mice used in the adoptive transfer studies, Villincre+mDELloxp mice were i.v. injected with 10-15x10^6 anti-CD43 depleted MACS (Miltenyi) purified splenic B cells from SW-HEL mice. For the TGFβ receptor inhibitor studies, before injection, cells were either left untreated or treated with DMSO or a TGFβ I/II receptor inhibitor for 2 hours and labeled with CTV, CFSE or eFlour670 (eBioscience). We used LY2109761 from Selleckchem.com at the concentration of 5μM per ml. Mice were sacrificed 1, 3 and 5 days later and analyzed by flow cytometry.

Histology: Spleen and PP were frozen and stored at -80^{o}C in Tissue-Tek O.C.T. Compound until ready for sectioning. 6-8 μm sections were fixed with acetone for 10 minutes at 4^{o}C and washed 3x with PBS at 5 minutes per wash. Slides were then blocked with PBS + 5% FBS for an hour at room temperature in a humidity chamber and subsequently stained with HEL-biotinylated and Bim APC for 2 hours at room temperature. The slides were then washed 3x with PBS + 0.5% Tween and stained with streptavidin Cy3, washed and mounted with Fluorogel. Slides were imaged using a Zeiss Imager M1 and Photoshop was used to overlay and edit images. For Haemotoxylin and Eosin (H&E) tissues with drop fixed in 10% Zinc Formalin. Tissues were embedded in paraffin and stained with H&E at the SBP histology core facility.

BrdU labeling: Mice were given 0.5mg/mL BrdU (Sigma) + 2% sucrose in their drinking water for 8 weeks and B cell turnover was measured by flow cytometry. Cells were harvested from spleen, pLNs, mLNs and PPs. Cells were stained with surface antibodies, fixed and then followed manufactures instruction for staining.

Flow cytometry staining: Spleen, pLN, mLN and PPs were isolated from mice euthanized with CO2. Organs were put into 10% FBS in PBS. 1-2x106 cells were stained with 0.2-0.5 μg of antibody in FACS buffer for 25 minutes and subsequently stained with secondary antibody when necessary. Abs used from eBioscience: anti-B220 (RA3-6B2), -CD86 (B7-2), -IgM(11/41), -CD69(H1.2F3), -CD95/Fas (J02) and -GL7 conjugated to APC, APC780, PE, FITC, PeCy7 or PerCp Cy5.5. To stain for HEL binding B cells, HEL bio (GeneTex) was used and revealed by using streptavidin-PerCpCy5.5, PECy7 or PE. Alternatively, cells were incubated with soluble HEL followed by anti-HEL biotinylated or anti-HEL (Rockland) and subsequently stained with either streptavidin or donkey anti-Rabbit FITC (Jackson), respectively. Anti-SMAD2 pS465/pS467 (072-670) was purchased from BD biosciences and mouse anti-TGFβR1 PE conjugated was purchased from R&D systems a biotechne brand. Live cells were identified using forward and side scatter. Data was acquired with a BD FACS CANTO using the FACS DIVA software (BD Biosciences) and data was analyzed using FlowJo (Treestar).

Anti-HEL flow assay: To detect HEL specific antibodies in serum and fecal extracts we modified sheep red blood cells (SRBCs) assay developed in our laboratory (25). Fecal extracts were dissolved in 1:1 ratio of PBS with protease inhibitor. HEL was conjugated to SRBC (46). Standard SRBC assay was then followed with HEL conjugated SRBCs to detect HEL specific anti-IgM, anti-IgG2, anti-IgG1 and anti-IgA antibodies (25).

Data analysis: All flow cytometry data was collected with BD FACS DIVA and analyzed using FlowJo Version 8.8.7.

Intestinal epithelial cell isolation: The intestine was removed and transferred into cold PBS. Intestinal contents were removed and the intestine was cut open longitudinally and washed in cold PBS. The tissue was then placed into a tube containing pre-warmed PBS containing 1mM DTT and shaken for 10 minutes at 180 rpm and 37^{o}C and then washed with PBS. The tissue was removed and incubated in HBSS supplemented with 1.5 mM EDTA for 15 minutes at 180 rpm and 37^{o}C. Tubes containing the tissue were vortexed for 1 minute and tissue was removed. Intestinal epithelial cells were centrifuged down to a pellet and resuspended in 1 mL of PBS. Cells were then filtered and either stained for flow cytometry or used for the lysozyme activity assay.

Transfection of HEK293T cells: HEK293T cells were either transfected with an empty MSCV-P2GM plasmid or MSCV-P2GM mDEL plasmid. 3µg of plasmid was added to 18µl of PEI and 172µl of DMEM and mixed gently. Plasmid was incubated at room temperature for 20 minutes before the addition of 2 mL of complete DMEM (10% FBS, 2mM L-glutamine, 100U/mL penicillin, and 100µg/mL streptomycin). HE293T cells were incubated plasmid for 2 days. Additional complete DMEM was added after overnight incubation and whole media changed 2 days post transfection. Cells were analyzed by flow on the third day by flow to check transfection efficiency.

Lysozyme activity assay: To analyze lysozyme activity, the EnzChek® Lysozyme Assay Kit (Molecular Probes) was used according to manufacturer's instructions, with modifications for testing on cells. Transfected HEK293T cells, isolated IECs and whole intestine sections were used for the assay. $5x10^4$ mDEL expressing cells or 8 mm sections of the small intestine of Villin^{cre+}mDEL^{loxp} mice were used. Fluorescence was measured using a fluorescence microplate reader with a fluorescein filter.

gDNA extraction: gDNA was extracted from fecal pellets collected from mice using a Qiagen QIAamp® Fast DNA Stool Mini Kit according to manufacturer's instructions with adjustments. Stool was collected into 2mL microcentrifuge tubes (Eppendorf). 1mL InhibitEX Buffer was added to each stool sample and vortexed until stool sample was homogenized. The suspension was heated to 95^{o}C for 10-15 minutes and vortexed for 15 seconds. Sample was centrifuged for 1 min and 600ul of supernatant was added to 25µl of ProteinaseK. 600ul of Buffer AL was added to the sample and vortexed for 15 seconds before it was incubated at 70^{o}C for 10 minutes. 600ul of ethanol was added to the lysate and mixed by vortexing. Lysate was added to the QIAamp spin column and centrifuged for 1 minute. Filtrate was discarded. Once all sample has been loaded onto column, 500ul Buffer AW1 was added to the column and centrifuged for 1 minute. The column was then washed with 500µl Buffer AW2 and centrifuged for 3 minutes. Column was centrifuged for 3 minutes and allowed to dry for 5 minutes at room temperature. To elute gDNA, 200ul of Buffer ATE was added to the column membrane and incubated for 2 minutes at room temperature before elution by centrifugation for 1 minute. Samples were stored at -20^{o}C.

RNA sequencing: HEL specific cells and non-HEL specific cells were FAC sorted in TRIzolTM Reagent (Invitrogen) from spleen, mLNs and PPs of Villin^{cre+}mDEL^{loxp}SW$_{HEL}$ and RVillin^{cre+}mDELloxp(BCL2) mice (100,000 cells in 500µl of TRIzolTM). RNA was isolated by the manufacturer's instruction. Purified RNA was further passed through the Qiagen RNA isolation kit column to remove any remaining residual. cDNA was synthesize using SMART (Switching Mechanism at 5' End of RNA template) technology and RNA sequencing was performed at genomics core of La Jolla Institute of Allergy and Immunology, La Jolla, CA. The data discussed in this publication have been deposited in NCBI's Gene Expression Omnibus and are accessible through GEO Series accession number GSE133159.

Statistics: All the graphs are generated using ELISA data, Flow and RT-PCR data were analyzed with Microsoft Office Excel and Prism 6. All the statistical analysis were done by unpaired student t test with 1 tailed or ANOVA for analyzing multiple groups. All the experiments were performed atleast 3 times unless specified in the figure legends.

Study approval: All animals were treated in accordance with the ethical standards set and approved by Sanford Burnham Preby's Medical Discovery, La Jolla, Institute's Institutional Animal Care and Use Committee.

Authors contributions: AS, CC, RCR designed the experiments; AS, CC, JJ, CRL, EK, NB, JRA conducted the experiments. AS, CC, JJ, WWL analyzed the experiment; AS wrote the manuscript: CL and EK helped in preparing the manuscript; JRA, RCR supervised the study.

Acknowledgements: We are thankful to Dr. David Nemazee at SCRIPPS Research Institute, La Jolla for providing BAFF transgenic mice. We acknowledge Buddy Charbono from SBP vivarium for performing all the injections and Alfredo Chavez, Andy Vasquez and Diana Sandoval for maintaining all mouse colonies. We are grateful to all the Rickert Lab members for providing feedback and suggestions during manuscript preparation. This research is supported by NIH R01 AI122344 to J.A and A.S. is the fellow of the Leukemia and Lymphoma Society.

References:

1. Eckburg PB, Bik EM, Bernstein CN, Purdom E, Dethlefsen L, Sargent M, et al. Diversity of the human intestinal microbial flora. *Science.* 2005;308(5728):1635-8.
2. Macdonald TT, and Monteleone G. Immunity, inflammation, and allergy in the gut. *Science.* 2005;307(5717):1920-5.
3. Fasano A. Leaky gut and autoimmune diseases. *Clin Rev Allergy Immunol.* 2012;42(1):71-8.
4. Macpherson AJ, and Uhr T. Induction of protective IgA by intestinal dendritic cells carrying commensal bacteria. *Science.* 2004;303(5664):1662-5.
5. Artis D. Epithelial-cell recognition of commensal bacteria and maintenance of immune homeostasis in the gut. *Nat Rev Immunol.* 2008;8(6):411-20.
6. Fubara ES, and Freter R. Protection against enteric bacterial infection by secretory IgA antibodies. *J Immunol.* 1973;111(2):395-403.
7. Gutzeit C, Magri G, and Cerutti A. Intestinal IgA production and its role in host-microbe interaction. *Immunol Rev.* 2014;260(1):76-85.
8. Suzuki K, Meek B, Doi Y, Muramatsu M, Chiba T, Honjo T, et al. Aberrant expansion of segmented filamentous bacteria in IgA-deficient gut. *Proc Natl Acad Sci U S A.* 2004;101(7):1981-6.
9. Brown EM, Sadarangani M, and Finlay BB. The role of the immune system in governing host-microbe interactions in the intestine. *Nat Immunol.* 2013;14(7):660-7.
10. Round JL, and Mazmanian SK. The gut microbiota shapes intestinal immune responses during health and disease. *Nat Rev Immunol.* 2009;9(5):313-23.
11. Mora JR, Iwata M, Eksteen B, Song SY, Junt T, Senman B, et al. Generation of gut-homing IgA-secreting B cells by intestinal dendritic cells. *Science.* 2006;314(5802):1157-60.
12. Mizoguchi A, Mizoguchi E, Takedatsu H, Blumberg RS, and Bhan AK. Chronic intestinal inflammatory condition generates IL-10-producing regulatory B cell subset characterized by CD1d upregulation. *Immunity.* 2002;16(2):219-30.
13. Song F, Wardrop RM, Gienapp IE, Stuckman SS, Meyer AL, Shawler T, et al. The Peyer's patch is a critical immunoregulatory site for mucosal tolerance in experimental autoimmune encephalomylelitis (EAE). *J Autoimmun.* 2008;30(4):230-7.
14. Uematsu S, Fujimoto K, Jang MH, Yang BG, Jung YJ, Nishiyama M, et al. Regulation of humoral and cellular gut immunity by lamina propria dendritic cells expressing Toll-like receptor 5. *Nat Immunol.* 2008;9(7):769-76.

15. Rosser EC, Oleinika K, Tonon S, Doyle R, Bosma A, Carter NA, et al. Regulatory B cells are induced by gut microbiota-driven interleukin-1beta and interleukin-6 production. *Nat Med.* 2014;20(11):1334-9.
16. Sattler S, Ling GS, Xu D, Hussaarts L, Romaine A, Zhao H, et al. IL-10-producing regulatory B cells induced by IL-33 (Breg(IL-33)) effectively attenuate mucosal inflammatory responses in the gut. *J Autoimmun.* 2014;50:107-22.
17. Gonnella PA, Waldner HP, and Weiner HL. B cell-deficient (mu MT) mice have alterations in the cytokine microenvironment of the gut-associated lymphoid tissue (GALT) and a defect in the low dose mechanism of oral tolerance. *J Immunol.* 2001;166(7):4456-64.
18. Nemazee D. Mechanisms of central tolerance for B cells. *Nat Rev Immunol.* 2017;17(5):281-94.
19. Cambier JC, Gauld SB, Merrell KT, and Vilen BJ. B-cell anergy: from transgenic models to naturally occurring anergic B cells? *Nat Rev Immunol.* 2007;7(8):633-43.
20. Yau IW, Cato MH, Jellusova J, Hurtado de Mendoza T, Brink R, and Rickert RC. Censoring of self-reactive B cells by follicular dendritic cell-displayed self-antigen. *J Immunol.* 2013;191(3):1082-90.
21. Wesemann DR, Portuguese AJ, Meyers RM, Gallagher MP, Cluff-Jones K, Magee JM, et al. Microbial colonization influences early B-lineage development in the gut lamina propria. *Nature.* 2013;501(7465):112-5.
22. Adams CL, Macleod MK, James Milner-White E, Aitken R, Garside P, and Stott DI. Complete analysis of the B-cell response to a protein antigen, from in vivo germinal centre formation to 3-D modelling of affinity maturation. *Immunology.* 2003;108(3):274-87.
23. Fischer MB, Goerg S, Shen L, Prodeus AP, Goodnow CC, Kelsoe G, et al. Dependence of germinal center B cells on expression of CD21/CD35 for survival. *Science.* 1998;280(5363):582-5.
24. Phan TG, Amesbury M, Gardam S, Crosbie J, Hasbold J, Hodgkin PD, et al. B cell receptor-independent stimuli trigger immunoglobulin (Ig) class switch recombination and production of IgG autoantibodies by anergic self-reactive B cells. *J Exp Med.* 2003;197(7):845-60.
25. McAllister EJ, Apgar JR, Leung CR, Rickert RC, and Jellusova J. New Methods To Analyze B Cell Immune Responses to Thymus-Dependent Antigen Sheep Red Blood Cells. *J Immunol.* 2017;199(8):2998-3003.
26. Gavin AL, Duong B, Skog P, Ait-Azzouzene D, Greaves DR, Scott ML, et al. deltaBAFF, a splice isoform of BAFF, opposes full-length BAFF activity in vivo in transgenic mouse models. *J Immunol.* 2005;175(1):319-28.
27. Thien M, Phan TG, Gardam S, Amesbury M, Basten A, Mackay F, et al. Excess BAFF rescues self-reactive B cells from peripheral deletion and allows them to enter forbidden follicular and marginal zone niches. *Immunity.* 2004;20(6):785-98.
28. Fu Y, Wang L, Xie C, Zou K, Tu L, Yan W, et al. Comparison of non-invasive biomarkers faecal BAFF, calprotectin and FOBT in discriminating IBS from IBD and evaluation of intestinal inflammation. *Sci Rep.* 2017;7(1):2669.
29. Vaux DL, Cory S, and Adams JM. Bcl-2 gene promotes haemopoietic cell survival and cooperates with c-myc to immortalize pre-B cells. *Nature.* 1988;335(6189):440-2.
30. McDonnell TJ, Deane N, Platt FM, Nunez G, Jaeger U, McKearn JP, et al. bcl-2-immunoglobulin transgenic mice demonstrate extended B cell survival and follicular lymphoproliferation. *Cell.* 1989;57(1):79-88.
31. Puthalakath H, Huang DC, O'Reilly LA, King SM, and Strasser A. The proapoptotic activity of the Bcl-2 family member Bim is regulated by interaction with the dynein motor complex. *Mol Cell.* 1999;3(3):287-96.
32. Wobke TK, von Knethen A, Steinhilber D, and Sorg BL. CD69 is a TGF-beta/1alpha,25-dihydroxyvitamin D3 target gene in monocytes. *PLoS One.* 2013;8(5):e64635.
33. Gros MJ, Naquet P, and Guinamard RR. Cell intrinsic TGF-beta 1 regulation of B cells. *J Immunol.* 2008;180(12):8153-8.

34. Cazac BB, and Roes J. TGF-beta receptor controls B cell responsiveness and induction of IgA in vivo. *Immunity.* 2000;13(4):443-51.
35. Bjarnadottir K, Benkhoucha M, Merkler D, Weber MS, Payne NL, Bernard CCA, et al. B cell-derived transforming growth factor-beta1 expression limits the induction phase of autoimmune neuroinflammation. *Sci Rep.* 2016;6:34594.
36. Snapper CM, Waegell W, Beernink H, and Dasch JR. Transforming growth factor-beta 1 is required for secretion of IgG of all subclasses by LPS-activated murine B cells in vitro. *J Immunol.* 1993;151(9):4625-36.
37. Zan H, Cerutti A, Dramitinos P, Schaffer A, and Casali P. CD40 engagement triggers switching to IgA1 and IgA2 in human B cells through induction of endogenous TGF-beta: evidence for TGF-beta but not IL-10-dependent direct S mu-->S alpha and sequential S mu-->S gamma, S gamma-->S alpha DNA recombination. *J Immunol.* 1998;161(10):5217-25.
38. Lebman DA, and Edmiston JS. The role of TGF-beta in growth, differentiation, and maturation of B lymphocytes. *Microbes Infect.* 1999;1(15):1297-304.
39. Spender LC, O'Brien DI, Simpson D, Dutt D, Gregory CD, Allday MJ, et al. TGF-beta induces apoptosis in human B cells by transcriptional regulation of BIK and BCL-XL. *Cell Death Differ.* 2009;16(4):593-602.
40. Wildey GM, Patil S, and Howe PH. Smad3 potentiates transforming growth factor beta (TGFbeta)-induced apoptosis and expression of the BH3-only protein Bim in WEHI 231 B lymphocytes. *J Biol Chem.* 2003;278(20):18069-77.
41. Wallace CH, Wu BX, Salem M, Ansa-Addo EA, Metelli A, Sun S, et al. B lymphocytes confer immune tolerance via cell surface GARP-TGF-beta complex. *JCI Insight.* 2018;3(7).
42. Dedobbeleer O, Stockis J, van der Woning B, Coulie PG, and Lucas S. Cutting Edge: Active TGF-beta1 Released from GARP/TGF-beta1 Complexes on the Surface of Stimulated Human B Lymphocytes Increases Class-Switch Recombination and Production of IgA. *J Immunol.* 2017;199(2):391-6.
43. Hadis U, Wahl B, Schulz O, Hardtke-Wolenski M, Schippers A, Wagner N, et al. Intestinal tolerance requires gut homing and expansion of FoxP3+ regulatory T cells in the lamina propria. *Immunity.* 2011;34(2):237-46.
44. Manicassamy S, Reizis B, Ravindran R, Nakaya H, Salazar-Gonzalez RM, Wang YC, et al. Activation of beta-catenin in dendritic cells regulates immunity versus tolerance in the intestine. *Science.* 2010;329(5993):849-53.
45. Eckmann JD, Chedid V, Quinn KP, Tse CS, Bonthu N, Nehra V, et al. P100 RITUXIMAB-INDUCED COLITIS: THE MAYO CLINIC EXPERIENCE. *Gastroenterology.* 2018;154(1):S51.
46. Paus D, Phan TG, Chan TD, Gardam S, Basten A, and Brink R. Antigen recognition strength regulates the choice between extrafollicular plasma cell and germinal center B cell differentiation. *J Exp Med.* 2006;203(4):1081-91.

Figure 1:

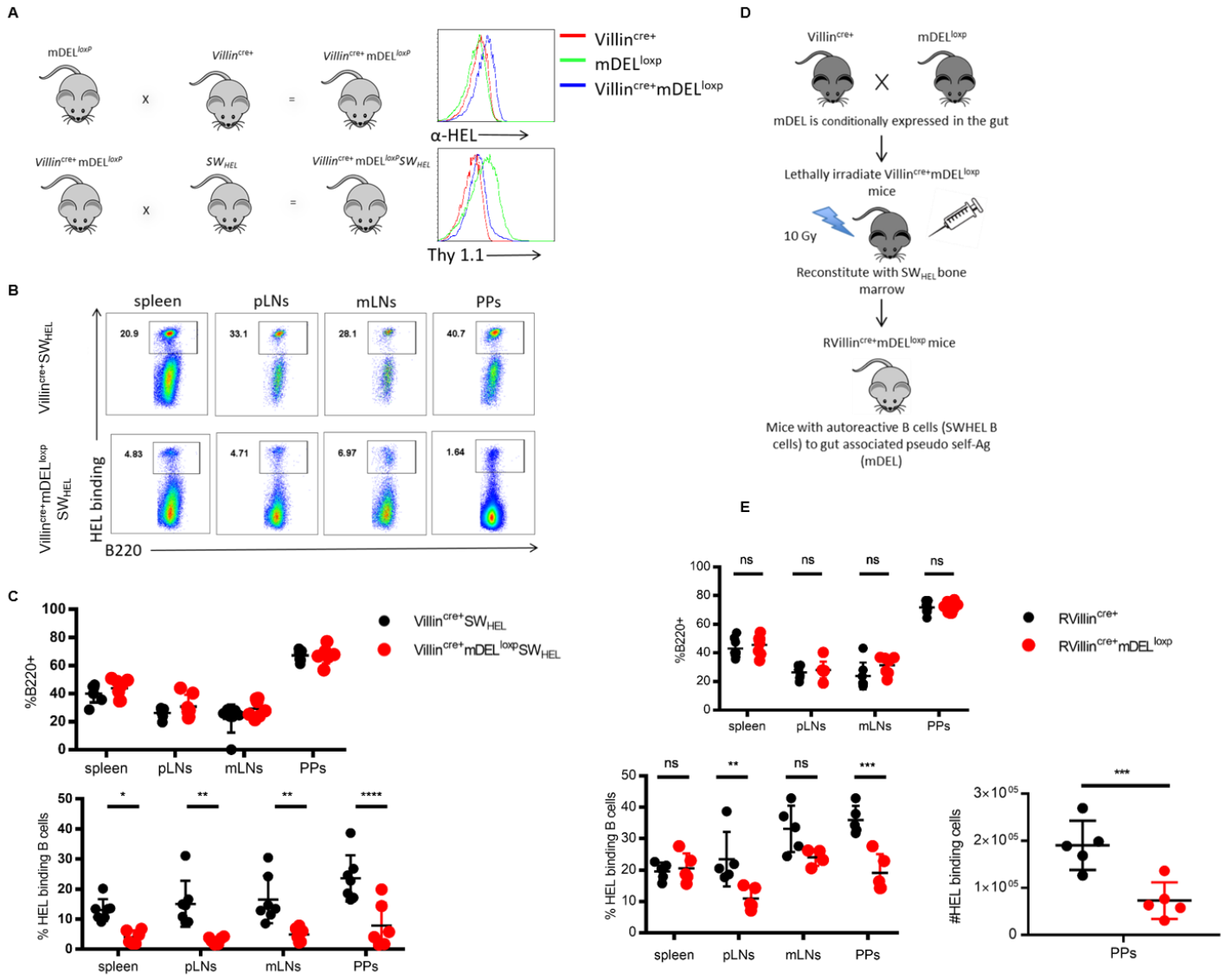

Figure 1: Self-reactive B cells diminishes upon gut associated antigen encounter: a) Left panel, breeding scheme to obtain Villin^{cre+}mDEL^{loxp}SW$_{HEL}$ mice. Right panel displays the gain of DEL expression and loss of Thy 1.1 upon Villin^{cre} recombination, measured by Flow cytometry. b) HEL specific cells population (gated on B220+HEL+) in spleen, pLNs, mLNs and PPs of Villin^{cre+}mDEL^{loxp}SW$_{HEL}$ and Villin^{cre+}SW$_{HEL}$ mice. c) B cells frequencies (gated on live cells, B220+) as analyzed by flow cytometry in spleen, pLNs, mLNs and PPs of Villin^{cre+}mDEL^{loxp}SW$_{HEL}$ and Villin^{cre+}SW$_{HEL}$ mice at the age of 6-8 weeks. d) Schematic of reconstitution experimental (RVillin^{cre+} and RVillin^{cre+}mDEL^{loxp} mice), data were analyzed using two-way ANOVA, was repeated more than 3 times. e) Top panel, graph of B cell percentages in Spleen, pLNs, mLNs and PPs and lower panel, HEL-specific cells percentages in spleen, pLNs, mLNs and PPs and absolute numbers of HEL-specific B cells in PPs isolated from RVillin^{cre+} and RVillin^{cre+}mDEL^{loxp} mice after 8 weeks post reconstitution, Data is representative of 3 mice per group, experiment was repeated more than 3 times and was analyzed using two-way ANOVA and grouped multiple T-test. **** is p<0.0001, ** is p<0.005, *** is p<0.001 and * is p<0.05

Figure 2:

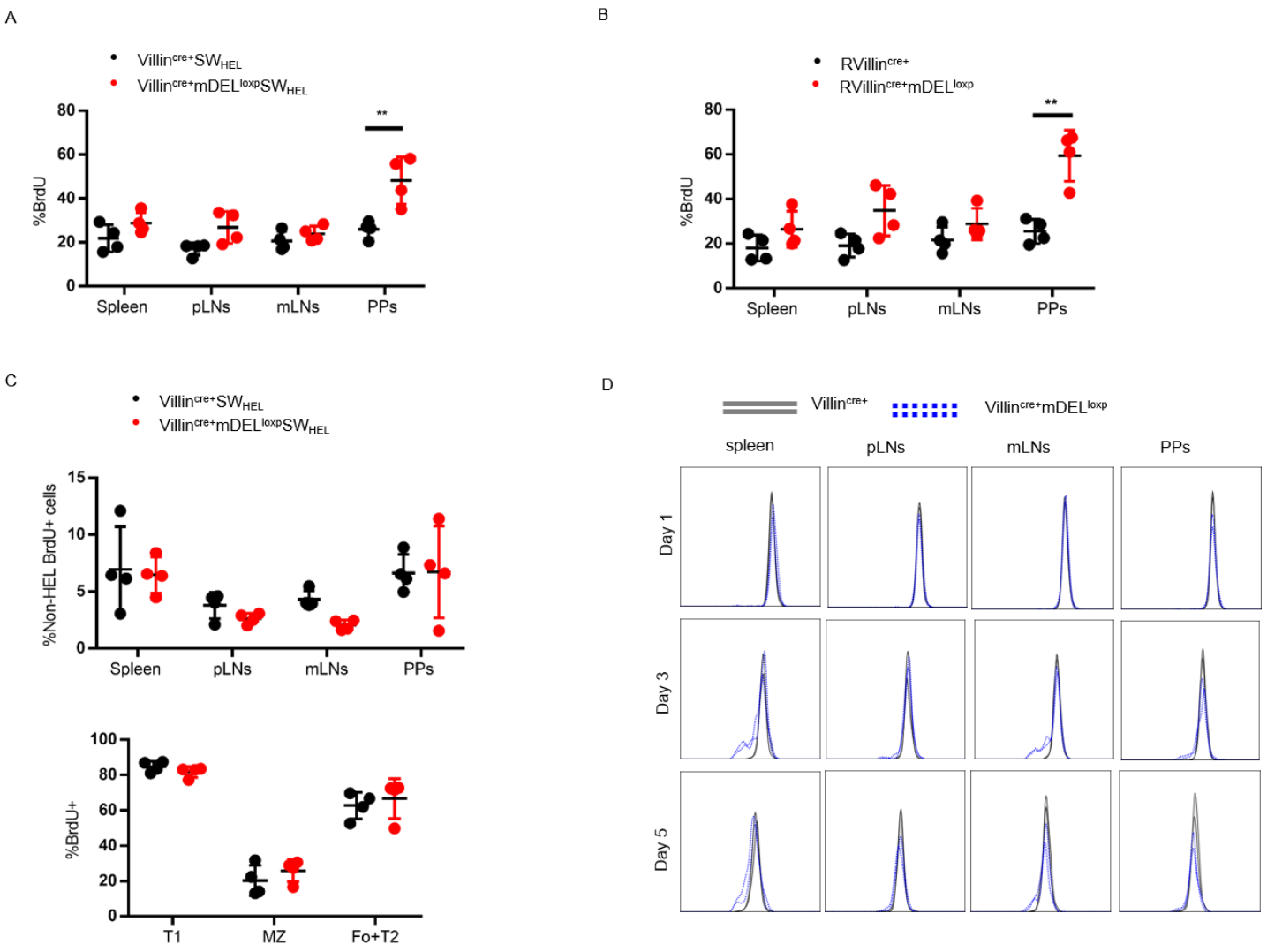

Figure 2: The pool of self-reactive B cells is renewed in gut by bone marrow: Mice were kept on BrDU containing water for 8 weeks post reconstitution. Newly formed HEL specific B cells (gated on lymphocytes, B220+, HEL+, anti-BrDU+) frequencies were measured by Flow cytometry in spleen, pLNs, mLNs and PPs of a) Villin^{cre+}SW$_{HEL}$ and Villin^{cre+}mDEL^{loxp}SW$_{HEL}$ and b) RVillin^{cre+} and RVillin^{cre+}mDEL^{loxp} mice. Data was analyzed by two-way ANOVA and grouped multiple T-Test. c) Frequencies of BrDU+ non-HEL-specific cells in spleen, pLNs, mLNs and PPs top panel and frequencies of BrDU+ HEL-specific T1, MZ, Fo and T2 B cells in spleen. d) Histograms displaying the MFI of eFluor670 to determine proliferation of adoptively transferred HEL specific B cells (gated on lymphocytes, single cells, eFluor670+, B220+, HEL+) in spleen, pLNs, mLNs and PPs into Villin^{cre+}mDEL^{wt} and Villin^{cre+}mDEL^{loxp} mice. Date is representative of two mice per group sacrificed on 1, 3 and 5 days post transfer were analyzed. Grouped statistical analysis was performed by multiple T-Test ** is $p<0.005$.

Figure 3:

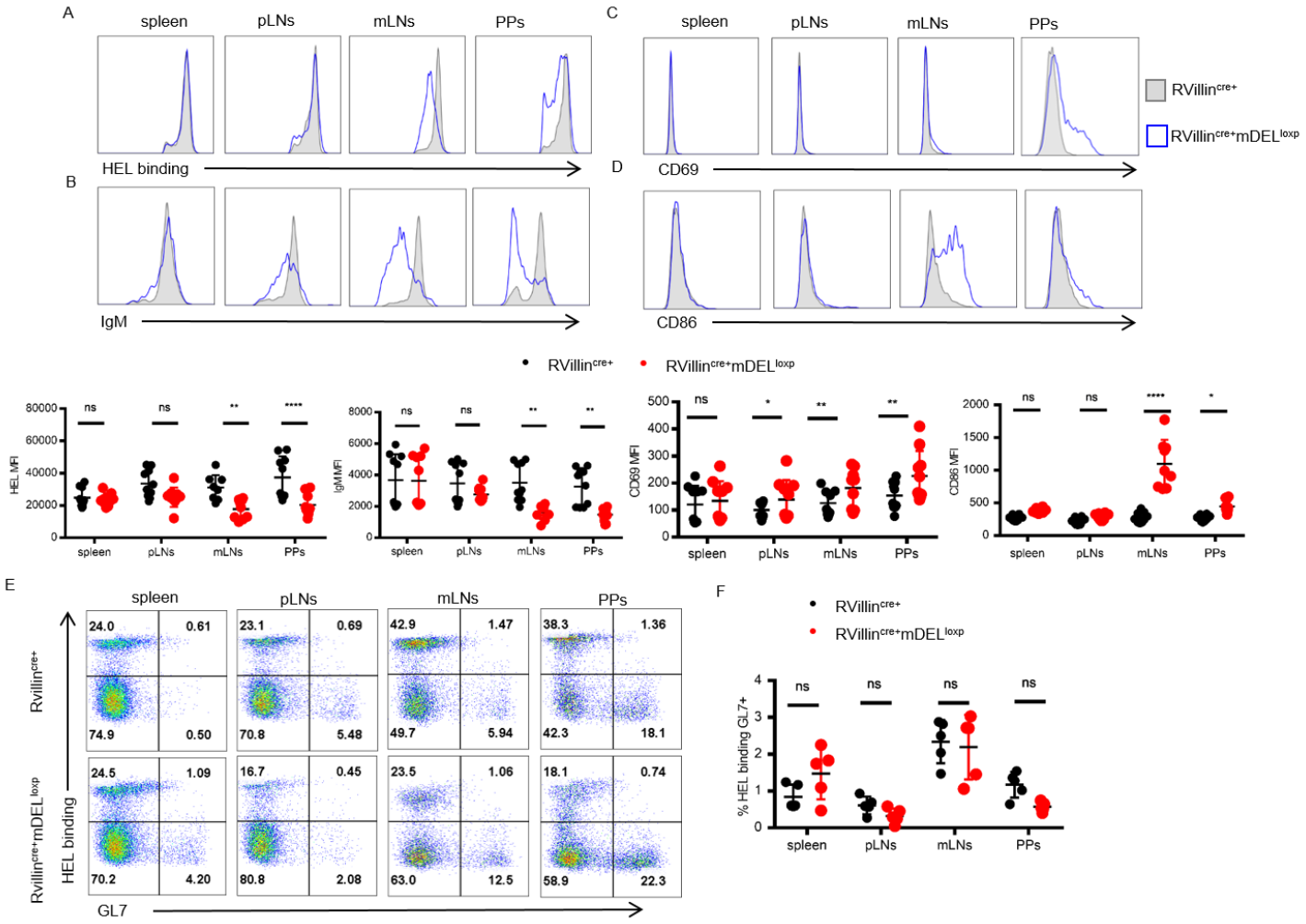

Figure 3: Self-reactive B cells gets activated upon antigen encounter in gut. HEL-specific cells were isolated from spleen, pLNs, mLNs and PPs of RVillin^{cre+} and RVillin^{cre+}mDEL^{loxp} mice. BCR density measured by MFI of a) HEL binding histograms of HEL-specific cells; below graph plot displaying the MFI of HEL binding of HEL-specific cells, b) anti-IgM histograms of HEL-specific cells; below graph plot displaying the MFI of IgM of HEL-specific cells from 8 mice per group. Activation of HEL specific cells was measured c) CD69 histograms of HEL binding; graph plot displaying the MFI of CD69. d) CD86 histograms of HEL binding left panel; graph plot displaying the MFI of CD86 in HEL-specific cells from 8 mice per group. e) Gated on B220+, dot plots of HEL specific cells (HEL+) and germinal center cells (GL7+) in spleen, pLNs, mLNs and PPs. f) Graph plot displaying GL7+HEL+ cells in spleen, pLNs, mLNs and PPs of 5 mice per group. Grouped statistical analysis was performed by multiple T-Test. **** is p<0.0001, ** is p<0.005, *** is p<0.001 and * is p<0.05

Figure 4:

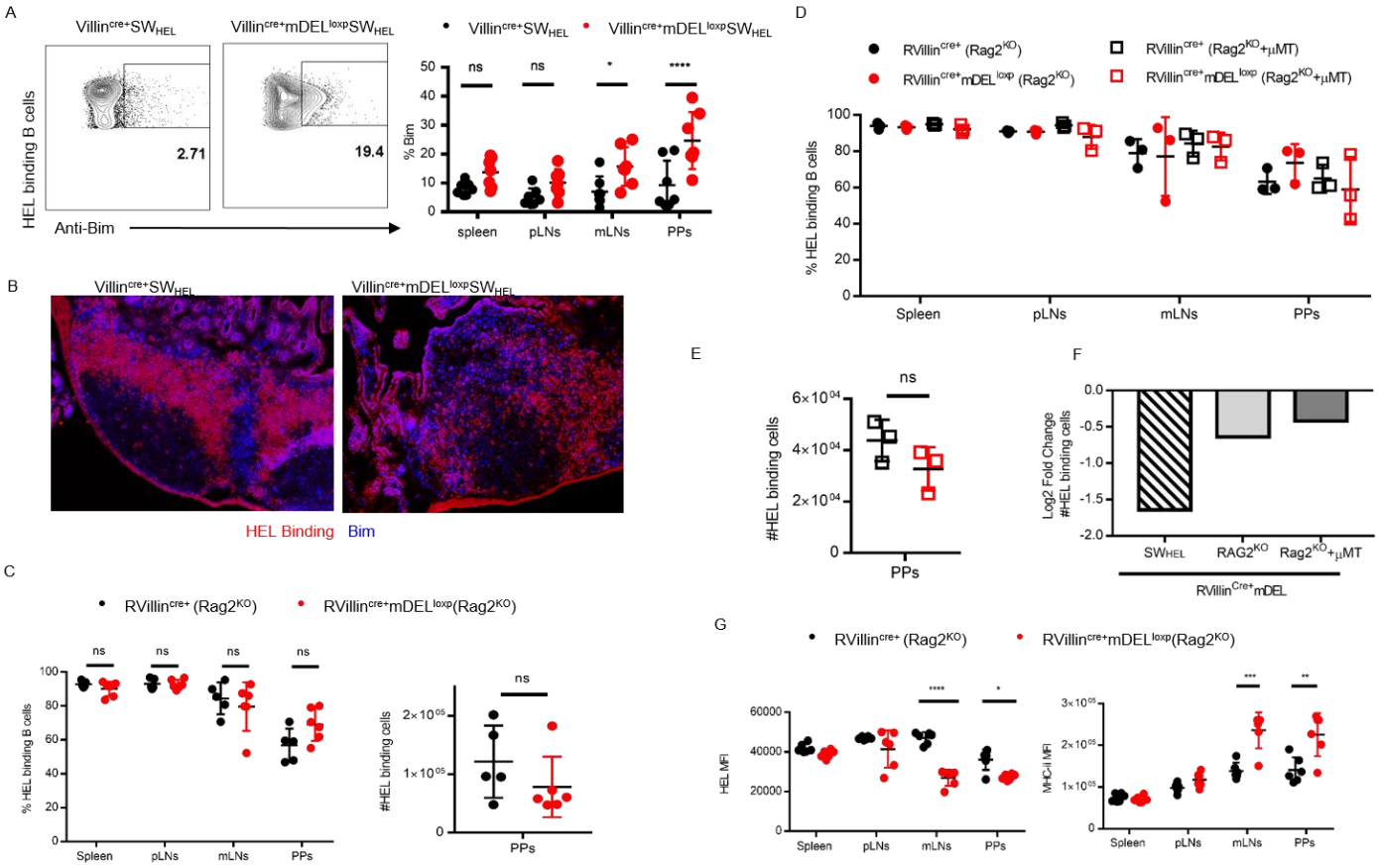

Figure 4: Self-reactive B cells undergoes Bim mediated apoptosis and Rag mediated receptor editing. a) gated on B220+HEL+ cells, dot plot displaying gain of Bim expression in HEL-specific upon antigen encounter in PPs, and graph displaying the %Bim+ HEL-specific cells in spleen, pLNs, mLNs and PPs from Villin^{cre+}SW$_{HEL}$ and Villin^{cre+}mDEL^{loxp}SW$_{HEL}$ mice. * is p=0.0442 and **** is p<0.0001. Data is representative of more than 3 experimental repeats and 7 mice per group. b) Displayed is the 20x image of immunohistochemistry staining of HEL binding (cy3) and Bim (cy5) of PPs from Villin^{cre+}SW$_{HEL}$ and Villin^{cre+}mDEL^{loxp}SW$_{HEL}$ mice. Villin^{cre+} and Villin^{cre+}mDEL^{loxp} mice were reconstituted with the bone marrow from SW$_{HEL}$Rag2^{KO} transgenic mice c) Graph displaying the frequency of B220+ cells in the spleen, pLNs, mLNs, and PPs and absolute numbers of HEL-specific B cells from PPs of RVillin^{cre+}(Rag2^{KO}) and RVillin^{cre+}mDEL^{loxp}(Rag2^{KO}) mice. d) Gated on B220+ cells, graph displays the frequency of HEL-specific cells in the spleen, pLNs, mLNs, and PPs of RVillin^{cre+}(Rag2^{KO}), RVillin^{cre+}mDEL^{loxp}(Rag2^{KO}), RVillin^{cre+}(Rag2^{KO}+μMT) and RVillin^{cre+}mDEL^{loxp}(Rag2^{KO}+μMT) mice. e) Graph displays absolute numbers of HEL-specific cells in PPs of RVillin^{cre+}(Rag2^{KO}+μMT) and RVillin^{cre+}mDEL^{loxp}(Rag2^{KO}+μMT) mice. f) Bar graph of log2 fold change in the numbers of HEL-specific cells from PPs of reconstituted Villin^{cre+} and Villin^{cre+}mDEL^{loxp} mice by SW$_{HEL}$, SW$_{HEL}$(Rag2^{KO}) and SW$_{HEL}$(Rag2^{KO}+μMT) bone marrow. g) Activation of HEL-specific from spleen, pLNs, mLNs and PPs of RVillin^{cre+}(Rag2^{KO}) and RVillin^{cre+}mDEL^{loxp}(Rag2^{KO}) mice by HEL binding MFI (left) and MHC-ii MFI (right). **** is p<0.0001, ** is p<0.005 and * is p=0.0253. Data is represented of 4 mice group was performed three for Rag2^{KO} rescue. Grouped statistical analysis was performed by multiple T-Test and Two-way ANOVA in Prism.

Figure 5:

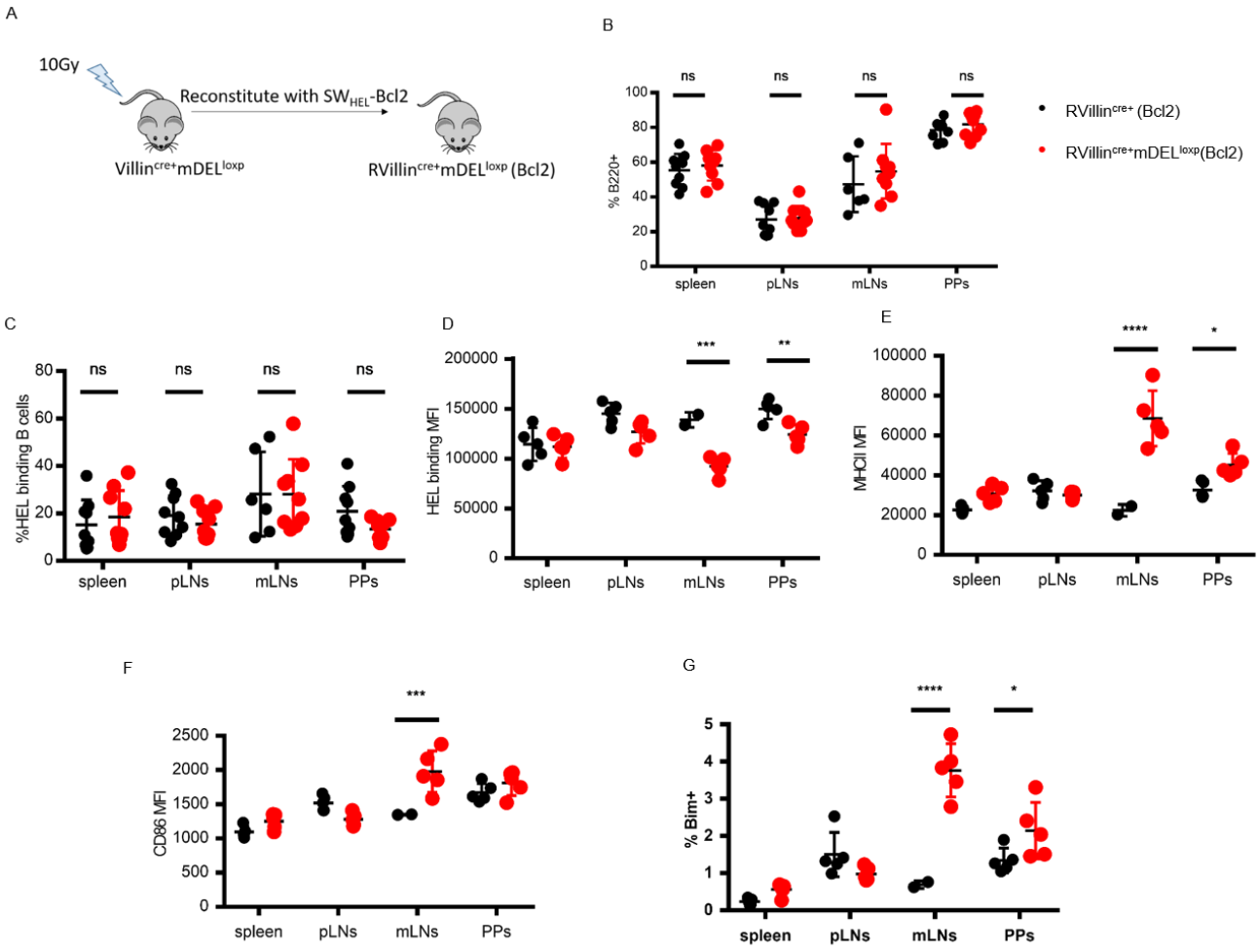

Figure 5: Ectopic expression of Bcl2 rescues the survival of self-reactive B cell in gut. a) Schematic for experimental design to reconstitute Villin^{cre+} and Villin^{cre+}mDEL^{loxp} mice with SW$_{HEL}$-Bcl2 transgenic mice bone marrow. b) Gated on lymphocyte population, displayed is the graph plot for frequency of B220+ cells in spleen, pLNs, mLNs and PPs of RVillin^{cre+} (Bcl2) and RVillin^{cre+}mDEL^{loxp} (Bcl2) mice. c) Gated on B220+ population, displayed is the graph plot for HEL binding cells frequencies in the spleen, pLNs, mLNs and PPs of RVillin^{cre+} (Bcl2) and RVillin^{cre+}mDEL^{loxp} (Bcl2) mice. MFI of d) HEL binding, e) MHC-ii, f) CD86 on HEL specific cells in the spleen, pLNs, mLNs and PPs of RVillin^{cre+} (Bcl2) and RVillin^{cre+}mDEL^{loxp} (Bcl2) mice. g) Gated on B220+Hel+ cells displayed is the graph plot of frequency of Bim+ cells. *** is p<0.001, ** is p<0.01, **** is p<0.0001 and * is p<0.05; n=9 mice per group. Grouped statistical analysis was performed by multiple T-Test.

Figure 6:

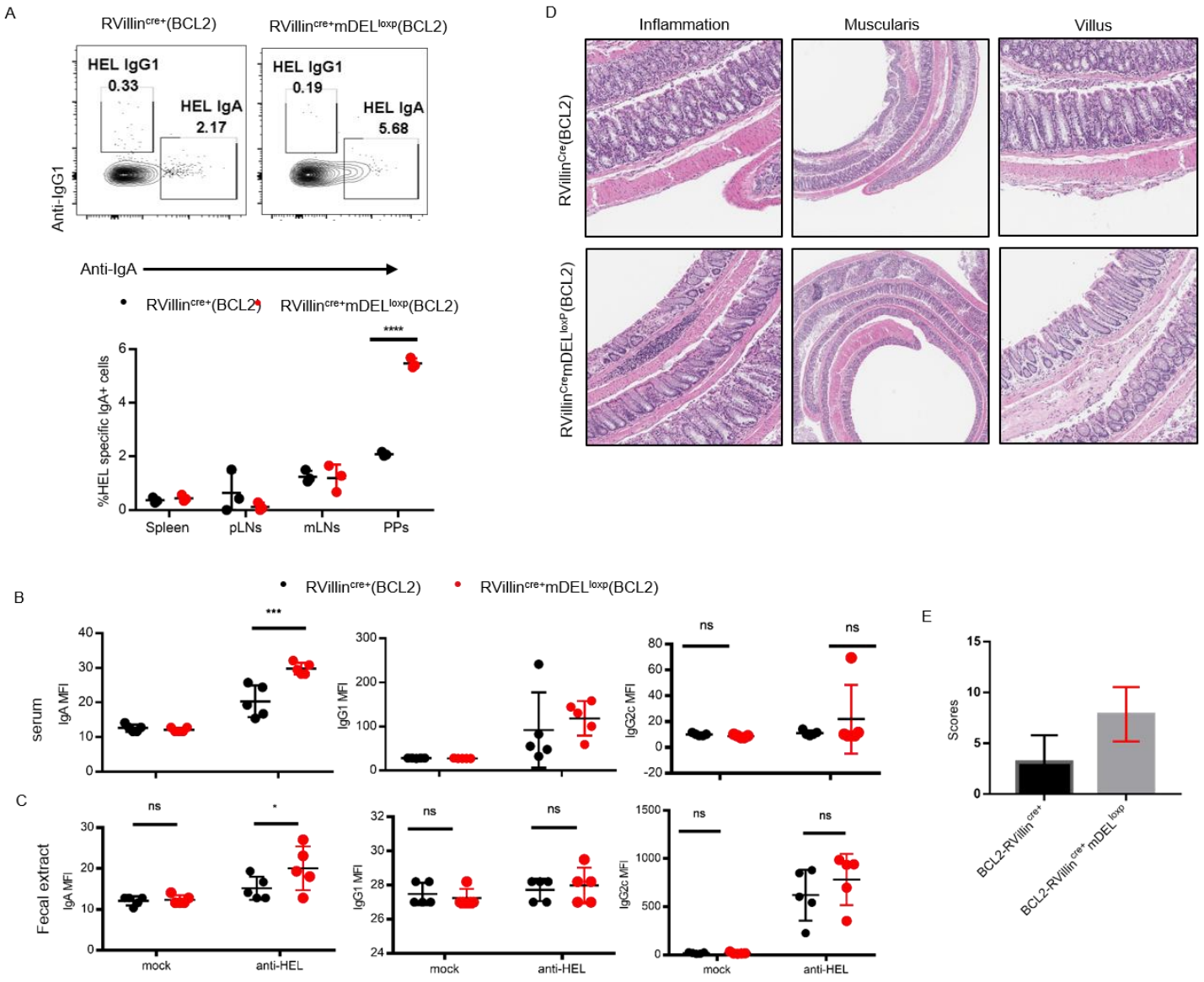

Figure 6: Deregulation of B cell tolerance in gut leads to IBD like disease. Flow contour plot showing the IgG1 and IgA switched HEL-specific cells in the PPs and Graph showing the frequency of HEL-specific IgA switched cells in the spleen, pLNs, mLNs and PPs of RVillin^{cre+}(Bcl2) and RVillin^{cre+}mDEL^{loxp} (Bcl2) mice. Graph plots showing MFI of HEL specific anti-IgA, anti-IgG1 and IgG2c b) in serum and c) in fecal extracts of RVillin^{cre+}(Bcl2) and RVillin^{cre+}mDEL^{loxp} (Bcl2) mice. d) H&E staining of small and large intestine showing infiltration and inflammation in RVillin^{cre+}mDEL^{loxp} (Bcl2) mice. e) Table illustrates the gut histological scoring of n=6 and n=7 respectively per group of RVillin^{cre+} (Bcl2) and RVillin^{cre+}mDEL^{loxp} (Bcl2) mice.

Figure 7:

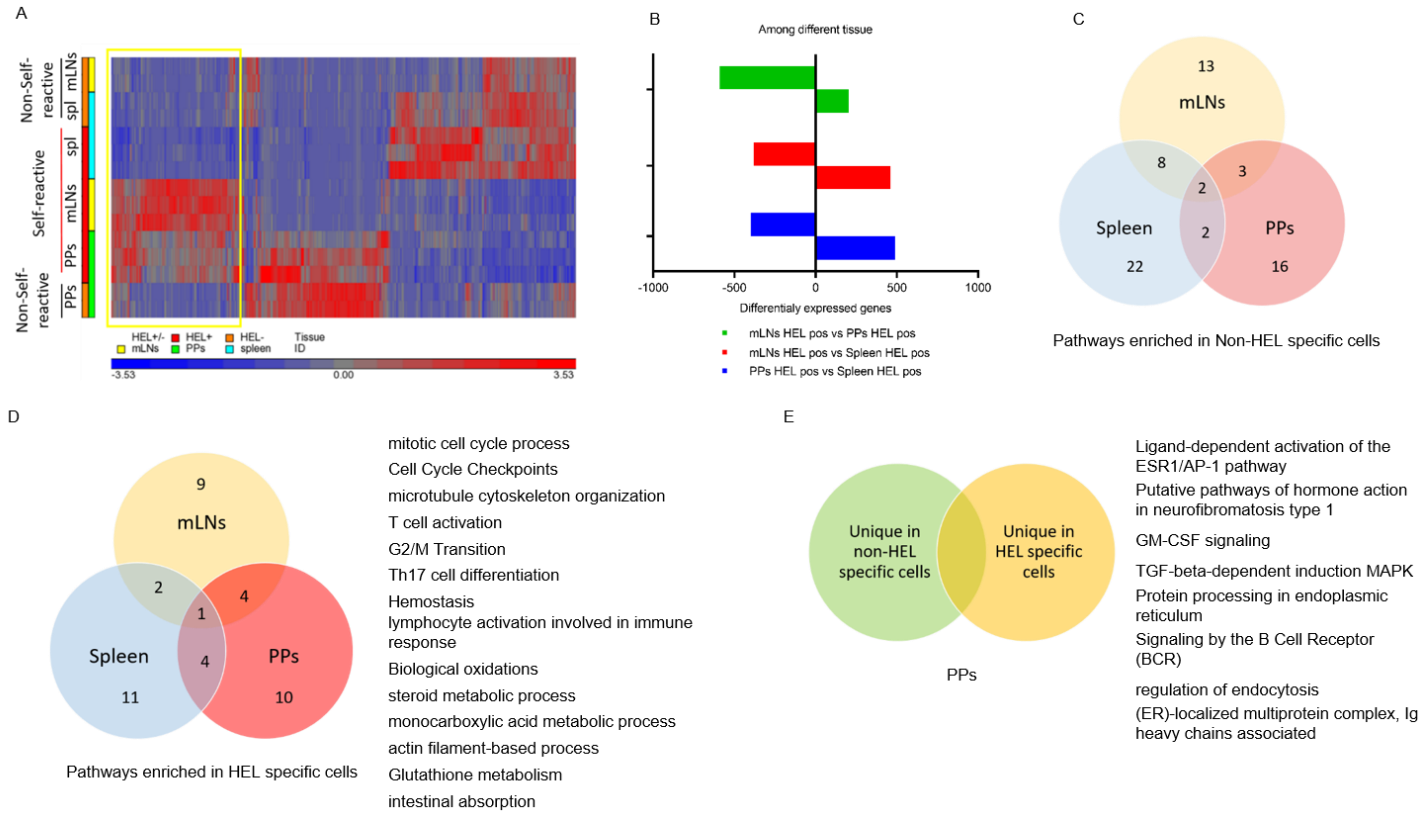

Figure 7: TGFβ signaling gets enriched in self-reactive B cells upon antigen encounter in PPs. A) Heatmap of supervised hierarchical clustering of differentially expressed genes (DEGs) in self-reactive B cells (HEL+ve) or normal B cells (HEL –ve) in Spleen, mLNs, and PPs isolated from Villin^{cre+}mDEL^{loxp}SW$_{HEL}$ mice. B) Bar graph showing the number of genes significantly (p=0.01) 1.5 fold over or under expressed in between self-reactive B cells from Spleen, mLNs, and PPs. Significant DEGs were run on metacore pathway analysis, C) Venn diagram of common or unique molecular pathways significantly ($p<0.05$) enriched in non-HEL specific cells isolated from Spleen, mLNs, and PPs; D) Venn diagram of common or unique molecular pathways enriched in HEL specific cells isolated from Spleen, mLNs, and PPs ($p<0.05$). Among the unique pathways identified in c&d in PPs E) is the Venn diagram of common or unique and list of unique molecular pathways enriched in non-HEL and HEL specific cells in PPs.

Figure 8:

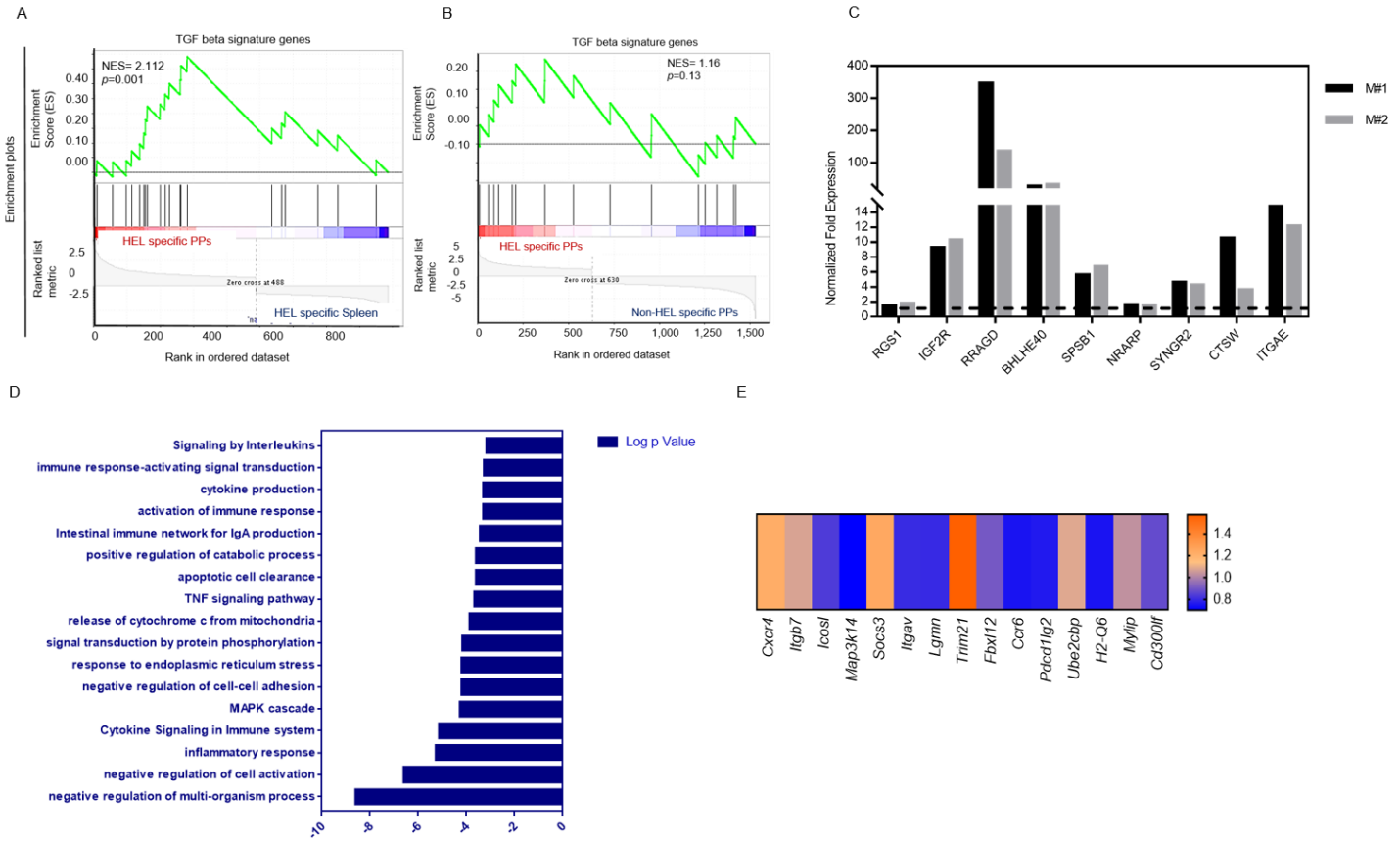

Figure 8: BCL2 induces an IgA immune network in self-reactive B cells. Gene set enrichment of TGFβ signature genes (GSE7460) A) in DEGs HEL specific cells from PPs vs Spleen, B) in DEGs HEL specific PPs vs non-HEL specific PPs. C) Graph showed Fold expression of 9 genes in HEL-specific cells from PPs of RVillin^{cre+} and RVillin^{cre+}mDEL^{loxp} mice (these genes were picked from TGFβ signature genes (GSE7460)). D) List of pathways enriched in HEL specific cells isolated from PPs of RVillin^{cre+}mDEL^{loxp} (Bcl2) verus HEL specific cells from isolated from PPs from Villin^{cre+}mDEL^{loxp}SW$_{HEL}$ mice. E) List of genes significantly overexpressed in log2 scale in PPs from RVillin^{cre+}mDEL^{loxp} (Bcl2) verus HEL specific cells from isolated from PPs from Villin^{cre+}mDEL^{loxp}SW$_{HEL}$ from Intestinal immune network for IgA production ($p<0.05$). n=3 HEL-specific samples, n=2 for non-HEL specific samples, and n=3 for RVillin^{cre+}mDEL^{loxp} (Bcl2).

Figure 9:

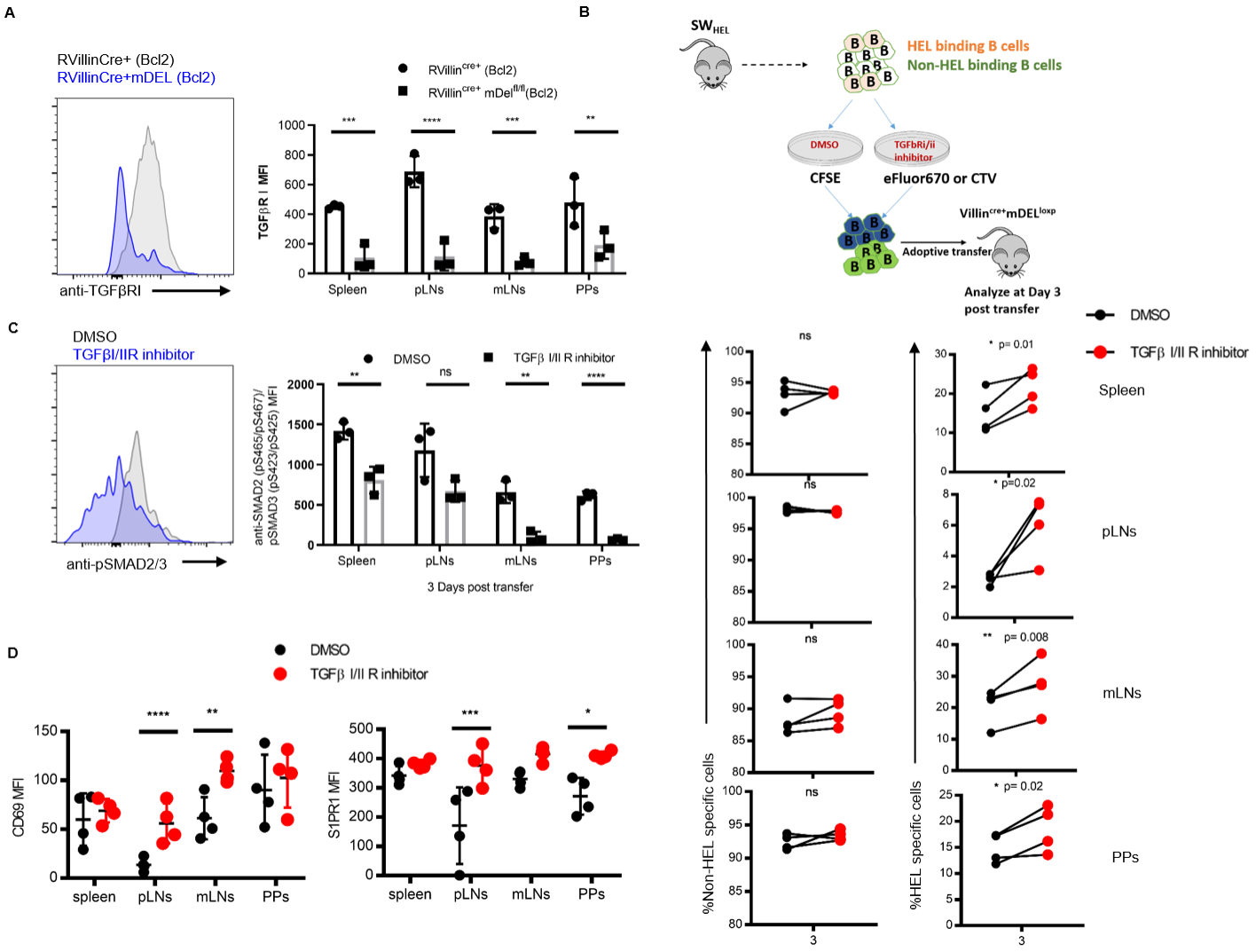

Figure 9: Inhibition of TGFβ signaling rescue self-reactive B cells upon antigen encounter in gut. A) Histogram and graph displaying the TGFβRI expressing and MFI of TGFβR1 staining in HEL-specific cells from spleen, pLNs, mLNs and PPs of RVillin^{cre+} (Bcl2) and RVillin^{cre+}mDEL^{loxp} (Bcl2) mice. B) Experimental design schematic to study the role of TGFβ signaling in self-reactive B cells. B) Gated on B220+ left panel shows the percentage of CFSE positive (non-HEL specific cells) and right panel shows the percentage of eFLuor670 positive cells in Spleen, pLNs, mLNs, and PPs. C) Histogram and graph displaying the p-Smad2/3 expression and MFI of p-Smad2/3 staining measured by flow in DMSO and TGFβI/II R inhibitor HEL-specific cells from spleen, pLNs, mLNs and PPs Villin^{cre+} and Villin^{cre+}mDEL^{loxp} mice, 72 hours post adoptive transfer. Graph of HEL specific cells treated DMSO or TGFβI/II R inhibitor in spleen, pLNs, mLNs, and PPs, D) of CD69 MFI and S1PR1 MFI. The statistical analysis was done by paired T-test in prism where, *** is p= 0.0002, ** is p=0.0077, * is p=0.0105, n=4 and experiment was repeated 3 times.